Histochemical and Electron Microscopic Studies on the Skin Disease Keratoderma Hereditaria Mutilans (Vohwinkel's Syndrome).

by

Sadhana Y. Ginde

Submitted in Partial Fulfillment of the Requirements

for the Degree of

Master of Science

in the

Biological Sciences

Program

School of Graduate Studies

Youngstown State University

September, 1999.

Histochemical and Electron Microscopic Studies on the Skin Disease Keratoderma Hereditaria Mutilans (Vohwinkel's Syndrome).

Sadhana Y. Ginde

I hereby release this thesis to the public. I understand this thesis will be housed at the Circulation Desk of the University Library and will be available for public access. I also authorize the University or other individuals to make copies of this thesis as needed for scholarly research.

Signature:

Sadhana Y. Ginde 9/13/99
Student Date

Approvals:

Paul C. Peters 9/13/99
Thesis Advisor Date

Gary R. Walker 9/13/99
Committee Member Date

Dina Fuegen 9/13/99
Committee Member Date

Peter J. Kasvinsky 9/16/99
Dean of Graduate Studies Date

Abstract

Keratoderma Hereditaria Mutilans (KHM) or Vohwinkel's Syndrome is a rare autosomal dominant skin disease characterized primarily by diffuse hyperkeratosis of both the palmar and the plantar regions of the skin. Other prominent features include an increase in the thickness of the stratum corneum layer of the epidermis, coupled with, an increase in the levels of β-glucuronidase enzyme in both serum and urine. It has now been established that Vohwinkel's Syndrome is a direct result of a defect found in the gene encoding a structural protein located within the cornified cellular envelope of the skin. This protein is known as loricrin. The exact chromosomal location of the specific loricrin gene was found to be in the 1q21 position, mapped within the epidermal differentiation complex (EDC). It is believed that a frameshift mutation within the loricrin gene causes a significant decrease in the flexibility of the cornified cell envelope layer by impairing and disrupting its ability to properly crosslink loricrin thereby contributing to an impairment in barrier function causing patients with Vohwinkel's Syndrome to retain water within the keratinocytes.

This research focuses on the exact nature of KHM with an emphasis on both transmission and scanning electron microscopy techniques, in addition to histochemical staining of epidermal tissues using various techniques. Immunohistochemical methodologies were employed for the identification and localization of the loricrin protein. Furthermore, experimental studies were performed to investigate and determine the specific role the ß-glucuronidase enzyme plays in this disorder by quantitatively determining the level of ß-glucuronidase and its localization throughout the layers of the epidermis via specific enzymatic assays.

The use of electron microscopy in this study provided a vital technique in which Vohwinkel's Syndrome was closely examined to reveal many insights into the nature and cause of this disease.

Acknowledgments

I would personally like to thank the following individuals: Dr. Diana L. Fagan, Dr. John Yemma and Dr. Gary R. Walker for their time and suggestions while evaluating this project and my thesis, and especially Dr. Paul C. Peterson for being my graduate advisor. His guidance, undying patience, support and time were very much appreciated. I cannot express in mere words how grateful and how thankful I truly am.

I would also like to extend my deepest gratitude and appreciation to Ms. Tamara Kerr of the Analytical Lab, Biology Dept. and Ms. Jeanette Killius of Northeastern Ohio University College of Medicine (NEOUCOM) for their help and expertise.

Special thanks goes to the Dr. Angela M. Christiano for her invaluable time, help, advice and suggestions. It was a pleasure to have met her. I would also like express my gratitude to the staff and laboratory technicians at the Pathology & Dermatology departments of Columbia University, College of Physicians & Surgeons in New York City. Their guidance and patience has been most appreciated.

I would also like to thank my family (see all that nagging finally did work!). And lastly, I would like to extend a special thank you to Mr. Bela Faltay for his time, patience, and understanding during this entire project. I wish him well.

I would be lost (even more so) without my faith in my religion to light the way down the right path. May that light always shine brightly!

Table of Contents

List of Figures

List of Tables

Introduction

In 1929, K. Vohwinkel described a mutilating form of diffuse hyperkeratosis of the palms and soles which he called KERATODERMA HEREDITARIA MUTILANS (KHM). In addition to palmar and plantar hyperkeratosis, patients with this disease present distinctive keratotic lesions characterized by a peculiar starfish-shaped or honey-combed shaped patterns (Sensi et al. 1994). In addition, many patients with KHM also exhibit ainhum-like or fibrous constrictions around the fingers and toes with the more severe cases leading to spontaneous amputations. This rare dermatological condition can occur in both sexes and its onset is usually during early childhood.

Vohwinkel's Syndrome (KHM) is a very rare and unique disorder of keratinization characterized by a distinctive histopathological and ultrastructural appearance. Routine laboratory investigations consisting of complete blood cell count (CBC), hepatic enzyme levels, renal function tests, serum protein and fasting blood sugar levels, as well as, systematic examinations are usually normal in most of these patients (Camisa and Rosanna, 1984). The teeth, oral mucosa, and nails are unaffected and appear normal. Radiographic x-rays of the hands and feet often reveal osteoporosis, demineralization of the bones, destruction of the interphalangeal joints, and tapering of the terminal phalanges (Presley and Bonte, 1981). Biopsy specimens of the affected areas usually demonstrate marked hyperkeratosis of the keratin layer (stratum corneum) with patchy hypergranulosis, large irregular keratohyalin granules which appear clumped in appearance, moderate acanthosis (spiny appearance) which is present in a very prominent granular layer, and the presence of some cells in the upper layers of the

epidermis with a highly vacuolated appearance (Krishnaram et al. 1986). In addition, the cellular nuclei appear extremely pyknotic or condensed and are usually absent in the more heavily damaged areas. Cell kinetic studies of the affected areas indicate an increase in the epidermal mitotic turnover of approximately six times normal (Klaus et al. 1970). The basal layers are normally intact and there are usually no significant changes present in the dermis.

The genetic origin of KHM is characterized as being autosomal dominant in nature. Congenital palmoplantar keratosis is rarely manifest at birth and is generally not recognizable until the ages of 3-4 years (Hatamochi et al. 1982). The hyperkeratosis usually begins as patches of epithelial thickening that grow and coalesce until they form thick, large, smooth, yellowish-white, translucent hard plates over the palms and soles. These well-defined, rough keratotic hard plates (also known as plaques) eventually become rigid and inelastic, predisposing them to the formation of fissures. The hyperkeratotic areas are generally surrounded by a 2 cm broad zone of an intensive erythroderma found on both the hands and the feet (Singh, 1986). Furthermore, hyperhidrosis soon develops, resulting in maceration and additional fissuring of the lesions. With maceration comes infection, and the hyperkeratoses lose their plate-like appearance and assume a dirty gray to brown color characterized by having a highly verrucous surface (Cole et al. 1984). Eventually, movement and tactile sensation are also severely restricted in these patients, as well as, loss of surface and thermal sensitivity. Unfortunately, once established, this condition persists throughout life.

The palmar lesions are usually the most severe in patients with KHM. They are often symmetrical in nature and consist of thickened epidermal plaques characterized by a yellowish-gray color. The increased thickness of the epidermis is usually between 0.5 cm to 2.5 cm depending on the severity of the case (Landazuri, 1991). This altered palmar epidermis usually does not exist as a single sheet, but is often divided by several deep fissures into blocks, creating a mosaic pattern in the lesion. In certain areas of the lesion, the edges of these plaques may be upturned revealing a red granular surface underneath. The lesions usually end abruptly at the wrists and on the sides of the hands in a narrow red marginal zone or border. The dorsal surfaces of the hands, as well as, the nails are usually unaffected. On the palmar surfaces of the fingers there exist plaques that are divided at the interphalangeal joints by transverse fissures which cause constriction of the digits. These constricting hyperkeratotic bands eventually lead to progressive strangulation and even mutilation of the digits. The constricting bands consist predominantly of a fibrous connective tissue of extremely high density closely resembling scar tissue. This results in a flexion deformity of the fingers interfering greatly with their movement and causing a great deal of pain and irritation for those patients afflicted with KHM. (Landazuri, 1991).

Unfortunately, patients with KHM suffer daily with very few options available with respect to a definitive treatment plan. Not only is there a great deal of excruciating pain involved, but restrictions in the movement of the affected hands and feet severely limits any routine daily activity. Basically, most cases of palmoplantar keratoderma are considered to be incurable. Once the hyperkeratotic process begins, it usually drags on chronically throughout the years with only short intervals of partial remission. Almost

every method of treatment so far proposed has been symptomatic usually providing only mixed results. Current treatment plans only slightly ameliorate the condition at best.

In the most severe of KHM cases, surgery is the only recognizable option available. In addition to the major complaints of pain and irritation, patients with severe KHM often display large fissures accompanied by hemorrhages whenever walking was attempted or whenever the disease was aggravated further by the interference of indeterminate factors (Kikuchi et al. 1976). Furthermore, many therapeutic and physiotherapeutic drugs available offered no positive results. Satisfactory results may be obtained when hormonotherapy (via synthetic hormones) is used but is never definitive and long lasting. The use of X-ray therapy is often quite disastrous, this besides increasing the keratoderma itself also produces very deep fissures, more abundant hemorrhages, necrosis and intense pain. Keratolytics and hot water baths usually have little or no effect. In such severe KHM cases, skin grafts via plastic surgery treatment often provides the best results (Kikuchi et al. 1976).

Fortunately, patients with more moderate cases of KHM may exhibit some degree of improvement with respect to treatments employing aromatic retinoid therapy. Retinoids, which are a synthetic derivative of Vitamin A, have proved to be quite effective in several disorders of keratinization. Earlier forms of treatment, prior to the advent of retinoids and their derivatives, relied on local keratolytic agents such as 20% salicylic acid or 30% urea applied topically with ineffective and unsatisfactory results (Albert et al. 1981). The synthetic retinoids are currently considered to be the drugs of choice in the treatment of a number of severe and chronic disease of keratinization. Etretinate (Tigason®/Ro 10-9359), a synthetic aromatic retinoid synthesized in 1942, is

currently the treatment of choice for patients suffering from KHM (Albert et al. 1981). Dramatic progress is usually seen in just 2 weeks after oral administration of Etretinate therapy (Albert et al, 1981). The hyperkeratotic lesions showed great improvement resulting in the appearance of normal looking skin, and in addition, any constrictions, swelling, erythema, and discoloration of the skin gradually disappeared over time resulting in the restoration of normal surface sensitivity. Biopsies of the treated skin revealed a greatly reduced stratum corneum with a significant decrease in epidermal hyperplasia. The effective dosage of Etretinate ranges anywhere from 0.6 mg/day to 30 mg/day depending on the severity of the individual case (Albert et al. 1981). Thus, a careful tailoring of the dose to the needs of the individual patient is necessary. Any further increase in dosage may cause unwanted side effects such as dry lips, dry eyes, conjunctivitis, drowsiness, epistaxis, redness of the face, fatigue, and moderate hair loss. In addition, an important pharmokinetic disadvantage of this compound is its storage in adipose tissue and extremely slow elimination from the body (Blanchet-Bardon et al. 1991). These side effects are directly related to the daily dose and could be altered by reducing the daily dose or placing the patient on an alternate day therapy. Surprisingly, lower dosages immediately lead to an increase in hyperkeratosis for unknown reasons.

The therapeutic effect of Etretinate is believed to be caused by a decrease in epithelial cell cohesion, as well as, an arrest in pathologic cornification (Duke et al. 1985). The primary factor underlying hyperkeratoses and pseudo-ainhum is an abnormal and excessive keratinization. It only seems likely that such pathologic cornification in KHM may lead to digital constrictions that can readily be reversed via oral Etretinate therapy. In addition, the administration of Etretinate has also resulted in a reduction of

the stratum corneum thickness, as well as, a significant decrease in the inflammation of the epidermis. Its metabolism occurs mainly in the liver and it is absorbed from the gastrointestinal tract. Etretinate exerts its optimal effects from between 2.5-5 hours after its administration (Cunliffe and Miller, 1984). The organic composition consists of ethyl (all E)-9-(4 methoxy-2,3,6-trimethylphenyl)-3,7-dimethyl-2,4,6,8-nonate traenoate. The organic structure of the derivative is as follows: (Goodman et al. 1994).

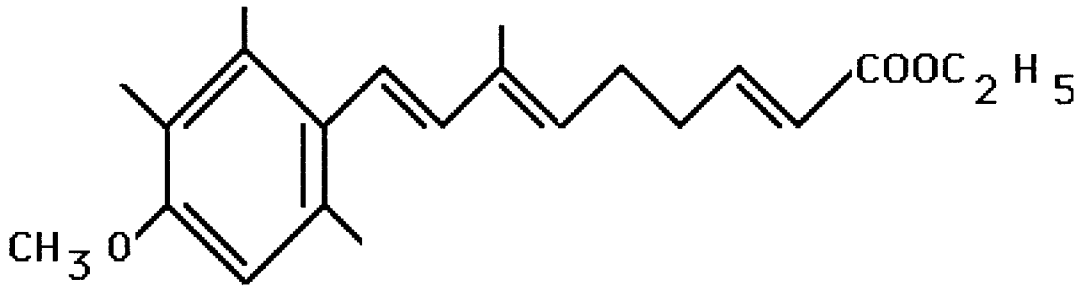

Studies have shown that cellular membranes have been targeted as one of the potential sites where retinoids are highly active. The hydrophobic structure of retinoids suggests that they will split into lipids once within these cellular membranes. The location of the retinoids within the lipid bilayers is an area that has unfortunately not been studied in great detail. A strong dipole interaction, however, does occur between the polar heads of the retinol and the phospholipids of the membranes (Iwahara et al. 1992). Further studies have also shown that the thickness of the water layer associated with the lipids at the monolayer-water interface was increased by the result of these interactions. Essentially, the retinol positions its ring upon the acyl chains, while its hydroxyl group projects outward along the head groups of the lipids into the aqueous environment. The retinoic acid does affect the bilayer of the membrane that is closest to the lipid-water interface. This effect is highly temperature dependent. At 45° C, the retinoid is placed higher within the membrane composed of lipid bilayers with its saturated acyl chains. At

much lower temperatures, such as 35° C, the retinoid is implanted in a much lower position within the membrane (Livrea and Packer, 1993).

Another possible target of retinoid action may be the immuno-competent Langerhans cell, which appear to be stimulated during retinoid therapy. These mitotic Langerhans cells are very rarely seen in normal epidermis and were not even observed in biopsies taken of diseased skin prior to retinoid treatment. Their increase during retinoid therapy could be of important clinical significance. The mitotic Langerhans cells are usually located suprabasally with several distinct visible chromosomes and a highly electron-lucent cytoplasm. A centriole with microtubules is often visualized as well; this being a definite characteristic of actively dividing mitotic cells (Kanerva et al. 1983). The mitotic Langerhans cells contain an abundance of short lamellae, endoplasmic reticulum, small mitochondria, coated vessicles and some lysosomes (Kanerva et al. 1983). There is also a noted growth in their population numbers, as well as, an increase in their stimulation within the dermis during retinoid treatment, it is thus possible that somehow these mitotic Langerhans cells are able to cross the basal lamina during retinoid therapy.

Retinoids are said to bind to their receptors by way of receptor proteins. Various researchers have identified such proteins as cellular retinol binding protein (CRBP), cellular retinoic acid binding protein (CRABP), and fatty acid binding protein (FABP) which are all synthesized by the liver (Smith, 1992). It is these retinoid receptor proteins that are responsible for specific responses such as cell differentiation or proliferation.

Aromatic retinoid therapy has greatly improved the lifestyle of many KHM patients. Prior to their advent, treatment for KHM consisted of local keratolytic agents

for mild-moderate cases and surgical intervention for the more severe cases. Many KHM patients that have undergone treatment with retinoids or their derivatives (Acitretin and Isotretinoin) have witnessed a dramatic improvement not only in the palmar keratoderma but also a significant decrease in the psuedo-ainhum as well. Etretinate has been proven to be a successful and safe treatment, but a daily maintenance dose is necessary to prevent recurrence. Although retinoids may not provide an absolute cure for these patients, it has at least been a step in the right direction.

I. *Skin*:

The skin is considered to be the largest organ found in the human body making up approximately 15-16% of an individual's body weight (Serri and Montagna, 1972). The human epidermis provides several different functions; the most important being, it serves as a barrier protecting the individual against injury and desiccation. In addition, the skin contains a variety of tactile sense organs that are able to receive stimuli from the external environment and lastly, it plays a significant role in the thermoregulation and water balance thereby influencing several of the body's metabolic functions.

The epidermis of the skin is composed of 5 very distinct and unique layers. The stratum basale (stratum germinativum) is the germinal layer that functions in the continual replacement of epidermal cells. It is composed of a single layer of cuboidal shaped cells that rest on the basal lamina. Next is the stratum spinosum (also known as the prickle cell layer) which is characterized by growing cells and the early stages of keratin synthesis. This layer is several cells thick and is characterized by polyhedral shaped cells containing several cytoplasmic processes. Thirdly, is the stratum granulosum layer which is distinguished by densely packed amorphous intracellular granules which contribute to the process of keratinization. This is the most superficial non-keratinized layer of the epidermis. The cells in this layer contain keratohyalin granules that are rich in amino acids (cysteine and histidine). The stratum lucidum is a thin homogeneous layer that is only found in thick skin, and lastly, is the most superficial layer known as the stratum corneum (cornified layer) which consists of flattened and fused cell remnants composed mainly of keratin, a fibrous protein. The process of

keratinization thus involves stem cells in the basal layer of the epidermis, which are capable of rapid proliferation over a long period of time, migrating upward to form the waterproof barrier of the skin (Mackenzie, 1969).

The epidermis varies in thickness throughout the body, ranging from 0.07 mm to 4.0 mm (Elias and Friend, 1975). The average thickness of the palms is approximately 0.8 mm and that of the soles is around 1.4 mm (Elias and Friend, 1975). These surfaces are subjected daily to increased pressure and friction so a thicker epithelium is required for their use. In human stratum corneum there are significant differences in structure and chemistry from one region of the body to another that are reflected in the skin's permeability. Plantar and palmar skin can be 400-600μ thick compared with 10-20μ for the back, arms, legs and abdomen (Elias and Friend, 1975). Despite its greater thickness, this tissue is a decidedly inferior barrier. Past studies have shown that weakly basic solutions, and even water in time, will dissolve plantar and palmar callus whereas the thinner stratum corneum from the other sites remains relatively unaffected (Baumberger et al. 1978). One of the major protective functions of the skin is derived from its uniquely low permeability. The part of the skin that contributes most to this protective role is the stratum corneum, the thin sheath of keratinized cells that comprises the outermost layer of epidermis.

Interest in skin permeability arises mainly from the capacity of the skin to limit the body's accumulation (or elimination) of substances by percutaneous transport. The epidermal skin barrier is the major factor in this process and can reduce overall rates of accumulation by several orders of magnitude. For example, most water-soluble, low-molecular weight non-electrolytes applied to the skin surface could diffuse into the

bloodstream approximately 1000x more rapidly if the epidermis were diseased, damaged or removed (Squier et al. 1978). Even with the skin intact, there are still 10,000-fold differences in the rates of penetration of different substances (Squier et al. 1978). The origin of the selective permeability of the skin and its quantitative prediction in terms of the relevant physical and chemical properties of the skin and the penetrating molecules are in essence the long-range purposes of the study of skin permeability.

The human epidermis is a dynamic system whose metabolic activity is regulated mainly by the integrity of the permeability barrier. This barrier resides specifically in the stratum corneum layer of the epidermis and comprises a unique 2-compartment system of structural protein-enriched corneocytes embedded in a lipid-rich intercellular matrix (Lampe et al. 1983). The water barrier relies specifically on these complex intercellular lipids which provide a major function by aiding in protection against loss of water and electrolytes. The lipid composition is as follows: ceramides (40%), cholesterol (25%), free fatty acids (25%), and lastly sphingolipids (10%) (Grayson and Elias, 1982). The strategic location of these lipids within the cellular interstices and their organization into membrane bilayers imparts impermeability to the epidermal tissue.

The stratum corneum, in addition to the stratum spinosum, provides the mechanical strength of the entire epidermis. The conversion of aqueous epidermal cells into dried, compact, keratin-containing stratum corneum cells is a crucial event in the continuously developing epidermis that largely determines and influences the low permeability character of the skin. Although considerable effort has been made to explore the mechanism whereby keratinocytes limit the diffusion of water, their participation in barrier function is not thoroughly understood. Keratinocytes are cells of

an extremely complex composition. Their cell walls are considered the most chemically resistant. The keratinocyte structurally consists of various submicroscopic filaments, an amorphous matrix and some remnants of cell organelles that are encased by a thickened and resistant plasma membrane. From a chemical viewpoint they can be considered to consist mainly of protein with some lipid and a small amount of carbohydrate. The current dilemma at hand is exactly which of these components possesses adequate properties to limit the diffusion of water through the epidermis.

The major result of the early work on the skin was the finding that the principal "barrier" function of the epidermis resides almost entirely in the stratum corneum layer, the thin coherent membrane of keratinized, epithelial cells that comprise the "dead" surface layer of the epidermis. The stratum corneum consists of approximately 15-20 layers of flat anucleate cells that are 10μ in width (Elias and Brown, 1978). It is essentially a heterogenous structure composed of protein-enriched corneocytes embedded in a lipid matrix. The most characterized components of the stratum corneum are keratins, specialized corneocyte proteins, lipids, specialized adhesion structures (desmosomes) and enzymes. The phenomenon of percutaneous absorption is essentially one of absorption onto the stratum corneum, diffusion through it and through the viable epidermis, and finally through the papillary dermis and into the micro-circulation. The viable tissue layers and the capillaries are relatively permeable and the peripheral circulation rapid so that for the great majority of substances, diffusion through the stratum corneum itself is rate limiting (Serri et al. 1972).

From previous work, it is clear that the stratum corneum acts like a passive diffusion medium. No active transport process across the skin has yet been demonstrated.

The passive nature of skin permeability is entirely consistent with the location of the major diffusion barrier in the stratum corneum, which consists of keratinized metabolically inactive cells (Elias, 1981).

The diffusional resistance of the skin is greatly dependent on its anatomy and ultrastructure. The composite structure of the skin permeability barrier is indicated by the three distinct layers (Grayson and Elias, 1982):

1). the stratum corneum (10μ)
2). a viable epidermis (100μ)
3). the papillary layer of the dermis (100-200μ).

Underneath this composite layer, lies the papillary arterial plexus, the site of epidermal micro-circulation.

The skin plays a highly integral role in the pathological process of those suffering from Vohwinkel's Syndrome. KHM patients are characteristically plagued with a peculiar abnormality found specifically in the water barrier layer of the stratum corneum. Basically, this permeability barrier is breached and the stratum corneum layer is distinguishable by an increase in water absorption and its sequestration (Camisa and Rosanna, 1984). This is most noticeable in thick skin (palmar and plantar surfaces), which under normal circumstances has an extremely dry, rough and sometimes scaly texture.

In relation to Vohwinkel's Syndrome, the hydration of the stratum corneum plays a very crucial and significant role. The stratum corneum is not immediately hydrated upon immersion in water. Although maceration may be detected in a few minutes, swelling continues fully for 3 days (Holbrook and Odland, 1974). The tissue can absorb

5-6 times its weight when fully hydrated and this water is strongly bound within the intracellular keratin (Squier et al. 1978). The diffusion of water and low-molecular weight, water-soluble molecules through this hydrated keratin is much more difficult than the corresponding free diffusion in aqueous solution. The filament-matrix ultrastructure is preserved under hydration and the water first appears to enter between the filaments and only later to diffuse within them. The hydrated intercellular keratin thus appears to comprise a stable 2-phase system at the macromolecular level: a continuous, water rich polar region intermingled with a network of non polar lipid. Hydration thus increases the thickness of the stratum corneum layer several fold.

The stratum corneum, the outermost protective layer of the skin, is the end product of epidermal differentiation and involves many biochemical processes. Awareness of the structural and biochemical complexity of this tissue is replacing old views of the stratum corneum as dead or inert. The same dynamic events that form the functional stratum corneum also expose it to pathological processes, including abnormal barrier function and hyperproliferation. Abnormalities in lipid composition and, to a lesser extent, protein composition are linked to stratum corneum pathophysiology. Alterations in stratum corneum lipid composition are often associated with perturbations of both barrier function, resulting in increased transepidermal water sequestration, and desquamation, resulting in a waxy, thickened, scaly stratum corneum as seen in cases of KHM.

TABLE 1:

COMPOSITION OF THE STRATUM CORNEUM:
(Taken from Squier, C.A. et al. 1978).

TISSUE COMPONENT	GROSS CHEM. CHARAC.	%
Cell membranes	Lipid & non-fibrous protein	5
Intercellular material	Lipid & non-fibrous protein	10
Cell contents	Lipid, 2	
	α-protein, 5	total
	ß-protein, 2	85
	non-fibrous protein, 1	

II. *The Water Barrier*:

The human skin plays a crucial metabolic role by virtue of the epidermis which constitutes a highly efficient barrier to the passage of water and other fluids. The water barrier of the skin is characterized by an aggregate of tightly adherent cells called keratinocytes, densely packed with lipid-enriched keratin fibrils to form a unique system. From previous studies on the skin, it is clear that the epidermis acts like a passive diffusion medium, no active transport processes across the skin has ever been demonstrated. This passive nature of skin permeability is entirely consistent with the location of the major diffusion barrier in the stratum corneum, which consists of keratinized metabolically inactive cells containing a keratin-phospholipid complex (Elias, 1981).

The complexity of the stratum corneum has unfolded over several decades. Originally thought to be several layers of simply dead cells, it is now considered to be a highly heterogenous and unique structure whose main role is to protect the individual from environmental changes. The major purpose of epidermal differentiation is to generate the stratum corneum, which also functions to protect the internal organs from desiccation. This purpose is achieved by the unique design of the stratum corneum at the cellular and molecular level and by its ability to respond to external injury through an array of metabolic processes (Onken and Moyer, 1963). The current theory regarding the true nature of the stratum corneum reveals that both barrier function and selective transport are subserved by the intracellular fibrillar-matrix complex of the stratum corneum cells themselves. The cells of the stratum corneum are largely devoid of any

organelles and consist of a dense tonofilament-amorphous protein matrix surrounded by a durable, sulfur-rich plasmalemma dense zone and a trilaminar plasma membrane (Wolff-Schreiner, 1987). Recent freeze-fracture and histochemical studies suggest that the stratum corneum is composed of lipid-depleted corneocytes embedded in a matrix consisting of neutral lipids and ceramides arranged in broad membrane bilayers (Goldsmith, 1989). Essentially, the barrier is composed of several layers of keratinized cells suspended in an extracellular lipid matrix.

The importance of stratum corneum lipids for barrier integrity has been appreciated for several decades. The stratum corneum barrier is formed by the subcellular organization of epidermal proteins and lipids into a 2-compartment model system of the epidermis with a continuous extracellular lipid matrix surrounding lipid-depleted, protein-enriched corneocytes. This 2-compartment model system of the epidermis is depicted below: (Elias and Brown, 1978).

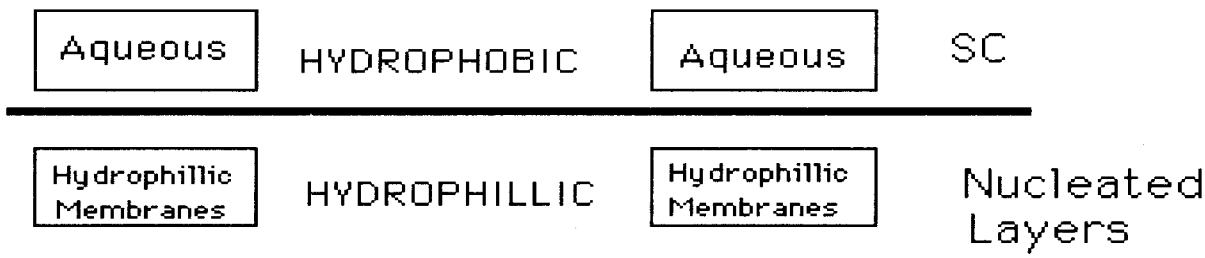

The above depicts the 2-compartment model system illustrating the localization of lipid-enriched domains to the stratum corneum interstices. The stratum corneum lipids are organized into multiple broad bilayers which lie between the corneocytes parallel to the plane of the skin's surface. These extracellular membranes appear to represent the barrier which prevents water loss. Essentially it is a continuous lipid phase surrounding a

discontinuous protein phase. This specific arrangement explains both the ability of the cells in the outer stratum corneum to take up water as the lipid-enriched bilayers act as semi-permeable membranes, as well as, the differences in the rates of percutaneous absorption of topically applied lipophilic VS. hydrophilic agents; the latter penetrating at a much slower rate. The overall stratum corneum water permeability is about 1000x lower than other biomembranes presumably due to its unique lipid composition (Squier et al. 1978). It remains to be seen whether the keratin filaments or the lipids play a greater role in the formation of the water barrier. In the past, penetration of polar molecules was presumed to occur near the outer surface of intracellular protein filaments while nonpolar molecules were thought to diffuse through the lipid matrix between the filaments (Scheuplein and Blank, 1971). Most researchers conclude that keratin merely forms a framework and the lipids are primarily involved in the barrier function.

The stratum corneum lipids are not only essential for the water barrier of the skin but also influence the activity of several key enzymes within the tissue important for stratum corneum maturation and desquamation. Variations in the levels and types of lipids present in the stratum corneum can influence stratum corneum barrier function, water content and skin condition. Stratum corneum lipids are known to be influenced by genetic variation, age, dietary influences, seasonal changes and environmental factors. These variations can lead to reductions in the levels of stratum corneum lipids and pre-dispose the individual to severe skin conditions.

Epidermal studies reveal that terminal differentiation of the epidermis eventually leads to desquamation, a process in which corneocytes are lost from the surface of the stratum corneum. Mechanically, this process is poorly understood. However, the

enzyme degradation of inter-corneocyte linking structures, or a reduction in inter-corneocyte binding forces, must occur to allow for cell shedding. Both the intercellular and covalently bound lipids may have a role in stratum corneum integrity.

It is now clear that the stratum corneum undergoes a series of alterations during its journey from the lower layers of the stratum corneum to the superficial layers, with each modification contributing to the overall properties of the stratum corneum. In addition, it is now known that these modifications are important for the three main functions of the stratum corneum: its barrier, mechanical and desquamatory properties. It is quite obvious that the barrier properties of the stratum corneum are highly dependent upon the levels and types of lipids within the stratum corneum. Any changes in lipid composition lead to changes in the properties of the lipids which may ultimately influence the water barrier.

Membrane permeability is thought to be determined largely by the lipid-protein structure of cellular membranes. The extreme sensitivity of the permeability barrier to damage by lipid solvents and the selective penetration of most nonpolar materials across the stratum corneum have long suggested that lipids are important determinants of skin penetration. The replacement of damaged cells from the surface of the skin with fresh undamaged corneocytes is a mechanism that ensures continual protection of the epidermis. As these new cells move up toward the outer layers of the stratum corneum, the cohesive forces between them are greatly reduced due to desmosomal degradation and lipid modifications. The desquamation process is now known to involve the degradation of surface lipids and protein species in the stratum corneum by various lipases, glycosidases and proteases. These key enzymes are involved in desmosomal

degradation, as well as, lipid degradation which are clearly dependent upon water for their activity.

The water permeability of the stratum corneum appears to be regulated primarily by the lamellar arrangement of lipid bilayers between the keratinocytes. The specific structural organization of these intercellular lipid lamellae is responsible for the very reduction in water of the skin and that these lipid-rich structures may also influence the process of desquamation in the stratum corneum. Studies have further concluded that substances which are lipid soluble (alcohols, ketones, etc.) penetrate the membrane barrier because of its lipid content, while uptake of water by the cell membrane protein provides entry for water soluble substances (Elias and Friend, 1975). The penetration of materials through the corneum depends on the state of cohesion between cells, as well as, the organization of intercellular lipid species. The lipids of the stratum corneum are critical for epidermal barrier function, but their origin and location remains in dispute. The intercellular lipid mix of the stratum corneum comprises four major fractions: free sterols, esterified sterols, free fatty acids, and sphingolipids (ceramides and glycosphingolipids) (Grayson and Elias, 1982). Previously done histochemical stains demonstrated the presence of neutral lipids in the stratum corneum intercellular spaces, phospholipids within granular cells, and PAS-positive material and between granular cells (Grayson and Elias, 1982). These combined histochemical and biochemical studies confirm that a definite shift from polar to neutral lipid does occur during the keratinization process. Recent data further concludes that these intercellular lipids are derived from epidermal lamellar bodies (also known as membrane-coating granules, keratinosomes, cementosomes or Odland bodies) (Elias, 1983).

Lamellar bodies are membrane enclosed organelles formed within the cells of the stratum spinosum and stratum granulosum layers. They may be further characterized as a type of lysosome. Lamellar bodies are organized into a continuous network by components of the cellular cytoskeleton. They are lipid-enriched and account for up to 25% of the overall cytosol volume (Elias, 1983). Their origins remain somewhat of a mystery but can tentatively be traced to either the smooth ER or the golgi. The lipid enrichment of the stratum corneum interstices results from the intercellular deposition of epidermal lamellar body contents, which are most likely hydrophobic and lipophilic in nature. After their initial secretion, the lamellar body contents undergo considerable remodeling into broad bilayers within the intercellular spaces during the final stages of keratinization. These intercellular spaces are approximately 20 nm spaces between the plasma membranes of adjacent keratinocytes (Elias, 1983). Thus, studies have conclusively shown that the structural basis for the epidermal water barrier appears to be due to the progressive accumulation of lamellar body material. Recent data further indicates that the stratum corneum forms a contiguous sheath of alternating squames and intercellular lamellae. The extruded contents derived from the lamellar bodies coalesces to form broad, laminated sheets within the epidermal stratum corneum (Myers, 1990). The subsequent upward progression of lamellar material throughout the interstices of the stratum layer probably explains the persistence of impermeability in the stratum corneum, as well as the normal resistance to percutaneous absorption.

Lamellar bodies measure 0.2 to 0.3 μm in diameter and are ovoid, secretory organelles that are synthesized within the spinous and granular cell layers (Elias, Goerke, and Friend, 1977). They appear to be packaged in the smooth endoplasmic reticulum.

They secrete their contents into the intercellular spaces at the base of the stratum corneum. The role of these lamellar bodies via their secretory process lies in the initial formation of the water barrier. They represent the putative source of almost all of the stratum corneum intercellular lipids. In addition to aiding in the formation of the permeability barrier, the lamellar body controls the availability of degradative enzymes responsible for the disintegration of corneocytes. These distinctive organelles are rich in sugars, glycosphingolipids, phospholipids, free sterols, cholesterol, and an array of hydrolases. These enzymes function in a dual capacity as they influence both barrier formation and desquamation. The specific contents of the lamellar bodies has been characterized as a homogeneous, electron-dense material containing possibly lipids, phospholipids, mucopolysaccharides and various enzymes including ß-glucuronidase, acid phosphates, proteases, lipases, non-specific esterases and presumably glycosidases. These contents presumably function in epidermal waterproofing. A second possible function of lamellar body enzymes may relate to desmosomal degradation. Although desmosomes cannot form a physiological barrier to water loss, they may contribute to the overall integrity of this tissue by mediating its cohesiveness. The internal structure of the lamellar body consists of a stack of parallel, electron-lucent discs enclosed by a limiting trilaminar membrane with a central interrupted striation separated by a somewhat thinner electron-dense band. The lamellar bodies thus appear to be compressed within the interior of the organelle ("pleated sheets"), and immediately after secretion these sheets begin to elongate within the intercellular spaces (Elias and Friend, 1975). This structural re-organization eventually gives rise to the basic lamellar unit structure of the stratum corneum.

The actual barrier effect has been postulated to be due to a physical sealing of the extracellular space by the extrusion of lamellar body contents. The consequence of lamellar body secretion is a massive exocytosis of materials resulting in the deposition of abundant lipid, enzyme, protein and undoubtedly other substances into the stratum corneum interstices, which is expanded by 10-15% of total volume (Elias, 1983). Thus, one could safely assume that any substances found within the individual lamellar bodies were subsequently released into the intercellular space where they could interact with both the intercellular substance and the cell membranes. Studies have confirmed that the lamellar contents actually impede, and ultimately block the outward movement of water soluble substances, substantially preventing access of these substances through the stratum corneum. The lamellar contents initially remain segregated in pockets, then fuse to form broad sheets which fill and greatly expand the intercellular regions of the stratum corneum. Further studies also indicate that the lamellar body contents are deposited on the outer surface of stratum corneum cells forming a prominent dense zone in freeze-fracture studies. Interestingly, this zone uniformly lines all cornified cells in the stratum corneum and may also function to impart rigidity to the individual cornified cells. Recent evidence indicates that the dense zone (approximately 250 A width) is also composed of a fibrillar and amorphous complex significantly different in chemical composition from keratin itself (Myers, 1990). In thin sections of freeze- fractured specimens, tonofilaments appear to arise within this zone further enhancing the stability of the intercellular lamellar network. Whether this may change the chemical composition and consequently the biological function of the stratum corneum cell membrane and secondarily the intercellular substance, is currently unknown.

The origin of the lamellar body is still somewhat of an enigma. Many researchers believe that these structures may arise from a granular matrix in the lower epidermal layers through a process of condensation and structural orientation within the organelles. The cytochemical demonstration of hydrolytic enzymes within the lamellar bodies has led to the conclusion that they belong to the lysosome cell line. The discharge of hydrolytic enzymes into the intercellular space has been interpreted to suggest that the enzymes are operative within the intercellular compartment, possibly by either altering the lamellae or the intercellular substance (Elias and Friend, 1975). This has led to the currently prevalent hypothesis that the enzymes are involved in the shedding of the epidermal cells (Myers, 1990). Many rare skin disorders including KHM, in which hyperkeratosis is a prominent feature, lend support to this hypothesis since they reveal an absence or significant reduction in the lamellar body population.

With the advent of electron microscopy and improved techniques for visualization, the lamellar body has received more attention in recent years. There is a general agreement that they have a highly organized lamellar internal structure. Likewise, most researchers agree that this highly organized structure relates to some special function, most likely the formation of the stratum corneum water barrier. However, the views are divided about their exact function. It had first been postulated that these lamellar bodies are sequestered in the upper granular layer into the intercellular layer where they disintegrate (Maltoltsy and Parakal, 1965). Other researchers have found that the number of lamellar bodies varies in the skin of different body regions. In areas where rapid desquamation took place, lamellar bodies were found to be the most numerous (Wilgram and Caufield, 1986). Thus, it can be postulated that lamellar bodies

are particularly numerous in conditions of rapid cell turnover and desquamation, such as the case with KHM. Taking into consideration all the findings obtained so far on normal and pathological skin, it can be assumed that the function of the lamellar body in some way is definitely related to the turnover of epidermal cells, and associated with it, to the rate of transformation of granular cells into keratinocytes. It is even further suggested that lamellar bodies may indirectly regulate the degree of shedding of epidermal cells (Wilgram and Caufield, 1986). Unfortunately, this is an area of research which has not provided many definite solutions. The true nature and function of the lamellar body still remains a mystery.

III. *The Langerhans Cell*:

The Langerhans cell (LC) is a large, elongated, suprabasal dendritic cell found within the epidermis. It is characterized mainly as a non-pigmented, independent and self-maintaining cell. Its presence can usually be seen at all levels below the upper stratum granulosum. More specifically, it is located within the suprabasal portion of the epidermis. Its mesenchymal origins are thought to give rise to its dendritic nature and its ultrastructural appearance is of a classical dendritic shape.

The LC is characteristically defined by its branched and tapering processes which extend from the cell itself and continue between the keratinocytes towards the granular layer, as well as, the epidermal-dermal juncture. Aside from being tapered, some of the dendritic endings appear almost expanded, resembling a "bouton" nerve ending. The LC is also thought to contain a variety of hydrolytic enzymes, although no research positively concludes this fact. Its true nature and function still remains somewhat of a mystery to researchers. Its general features includes a plasma membrane which exhibits no desmosomal contacts with adjacent keratinocytes. In addition, no tight junctions or gap junctions have been observed as well. It can further be distinguished by its highly indented and irregularly shaped nucleus, which may often be lobulated or even convoluted. It does however, contain all the characteristics of a metabolically active cell engaged in protein synthesis.

The Langerhans cell has been an integral part of epidermal studies for more than a century. The cell has managed to elude researchers for years and continues to remain much of a mystery regarding its true nature and function. Unfortunately, with regards to

the pathological process of KHM, this mystery remains unsolved. The Langerhans cell population is greatly decreased in most human skin diseases, although their frequency seems to be greatly increased in disorders involving abnormal keratinization (Stingl, 1980). This is true in most of the KHM cases as well. Many cases of KHM patient demonstrate an abnormally high population of vitally active mitotic LC which may play a significant role in the pathological process of this disease, although their precise role and function has yet to be determined (Camisa and Rosanna, 1984).

Since these cells cannot be identified in routine hematoxylin-eosin sections, special staining techniques are required for their visualization using light microscopy. LC contain various hydrolytic enzymes, such as acid phosphatase and ß-glucuronidase, which permit their identification by specific enzyme-histochemical techniques (Wolff, 1972). The stain of choice for the visualization of LC is via the ATPase staining technique. The recognition and identification of LC using electron microscopy demonstrates a clear cytoplasm devoid of tonofilaments, desmosomes and melanosomes. In addition, the presence of a distinctive cytoplasmic organelle which is now referred to as the "Langerhans cell granule" (or Birbeck granule) provides reliable positive identification (Shelley and Lennart, 1978). Specifically, the Langerhans cell granule usually appears as a rod-shaped organelle of variable length and position. It exhibits different morphologic features in different planes of sections but between the limiting membranes there is a linear density with a periodic striation that gives the rod a "zipper-like" appearance (Shelley and Lennart, 1978). The granules are distributed at random within the cytoplasm but often are seen in close proximity to the Golgi region. They also may occur at the cell periphery and some even demonstrate a continuity with the outer

cell membrane. Freeze fracture replica studies of the LC granule confirms that the paracrystalline character of its membrane suggests a protein nature (Wolff, 1972). The origin and function of this granule still remains somewhat of a mystery. Many researchers believe that the elusive granule may be a result of an infolding of the cell membrane. This hypothesis further suggests that the villi fold inward on themselves, thus creating the rod or actual plate structure which detaches and moves within the cell (Bassett, 1976). Other researchers conclude that the granules arise as vesicles in the Golgi apparatus and with maturity, they assume a rod-like extension which moves toward the cell periphery (Hashimoto and Gross, 1971).

The electron microscope studies of the LC reveal several distinguishing characteristics. The LC possesses a clear cytoplasm containing a highly lobulated nucleus. In addition, it appears to be devoid of any desmosomes and tonofilaments. The cytoplasm of the LC contains all the characteristics of a metabolically active cell engaged in protein synthesis. The number of free ribosomes may vary in number but in most cells they are rather numerous, this leads to an increase in the overall density of the LC cytoplasm which appears to exceed that of adjacent keratinocytes (Shelley and Lennart, 1978). Such cells have often been referred to as "dark Langerhans cells" (Shelley and Lennart, 1978). These "dark" LC are most prominent in disease states, such as KHM, although their exact nature has yet to be determined (Camisa and Rosanna, 1984). It has been postulated that the increased density of such "dark" Langerhans cells is the result of a condensation of their cytoplasm due to extracellular pressure. It consists of typically stacked cysternae which are often dilated and of multiple small vesicles at its concave face and lateral margins. In addition, the cytoplasm contains a variety of vesicles of

various sizes- some of which exhibit a "fuzzy coat" on their internal surface of their membrane. This "fuzzy coat" is thought to represent cross sections of the vesicular portions of the LC granules. The presence of oblong granules with a dense matrix and a trilaminar limiting membrane has also been seen in LC, although their presence is often quite rare (Wolff, 1972).

Langerhans cells contain a variety of single membrane limited dense bodies containing various hydrolytic enzymes such as acid phosphatase and ß-glucuronidase. These dense organelles have recently been characterized as lysosomes. Lysosomes are not necessarily present in every LC but they may be quite numerous. They are lined by a single triple- layered membrane and contain a granular matrix, lamellae and whorled membranes, which are myelin-like structures (Ebner, 1977). In addition, LC also exhibit multivesicular bodies which may play a significant lysosomal role. It has further been suggested that the Langerhans cell contributes to the autolytic phase of keratinization by promoting the concentration of hydrolytic enzymes (such as ß-glucuronidase) in the granular layer (Shelley and Lennart, 1978). Langerhans cells are evenly distributed throughout the epidermis and its frequency is approximately 100 cells/mm squared in 2 week old epidermis. After 4 weeks, with increased thickness of the granular layer, the frequency of LC is also increased to 400 cells/mm squared. With keratinization, LC frequency is increased to 800 cells/mm squared. In contrast, after keratinization is complete, the LC frequency drops significantly (Kustula and Orci, 1978).

It is quite clear that a definite relationship does exist between the density of the Langerhans cells and the degree of keratinization. This conclusion may also help to explain the regional variations of LC cell counts in human epidermal studies. Previous

observations have indicated that the LC population is more numerous in the thicker regions of epidermis (palmar and plantar skin), as well as, their increased presence in disease states (Hutchens et al. 1971).

It has repeatedly been suggested that the Langerhans cells regulate keratinocyte differentiation and proliferation and in fact, LC are confined to epithelia which are squamous in nature and which have the capacity to keratinize. Furthermore, in certain disease states such as Vohwinkel's Syndrome, there exists a definite relationship between LC frequency and degree of keratinization (Stingl, 1980). In addition, within such diseased epidermis, the LC was clearly identified as a highly differentiated cell capable of proliferation. The granules themselves appeared to be much more numerous and long, filling not only the cytoplasm, but also emerging within the nucleus, as well as, outside the cell (Shelley and Lennart, 1978).

It is quite obvious that the recent developments in this area of research have raised a host of several questions which at this time cannot be answered but they clearly do indicate the direction in which Langerhans cell research will be pursued in the future.

IV. *Beta-Glucuronidase Enzyme*:

Beta-glucuronidase is an enzyme that is widely distributed within various human tissues and body fluids. Its primary role is to act as a catalyzer in the hydrolysis of glucuronic acid esters of alcohols, phenols, certain carboxylic acids, steroids, and bilirubin. ß-glucuronidase is highly abundant in the liver, kidney, spleen, pancreas, and other vital tissues including the skin. It has been suggested that the activity of this particular enzyme reflects the degree of cellular proliferation taking place in a tissue or organ (Rutenberg et al. 1973). An increase in its circulating concentration provides great clinical significance in many types of pathological processes, including KHM. Thus, a definitive relationship between ß-glucuronidase and proliferative activity does indeed exist.

ß-glucuronidase is an acid hydrolase, most commonly found within the lysosomes of the epidermis. It is classified as a tetrameric glycoprotein composed of four identical subunits. In addition, ß-glucuronidase is also involved in the breakdown of hyaluronic acid which is a major component of ground substance found in the dermal layers of the skin (Dingle et al. 1979). More specifically, ß-glucuronidase acts in the acidic environment of the lysosome as an exoglycosidase to remove terminal ß-glucuronic acid residues from the non-reducing end of glycosylaminoglycans and other glyco-conjugates. Mammalian ß-glucuronidase has a broad pH optimum ranging between 3.8-5.0 (Noriega et al. 1993). One of the more prominent features seen in most patients with Vohwinkel's Syndrome is an extremely elevated level of serum ß-glucuronidase enzyme activity (Camisa and Rosanna, 1984). The presence of hyperkeratotic and hyperplastic epidermis

seen in KHM patients, with a lack of characteristic inflammatory infiltrate and dermal pathology suggests an epidermal source for the elevated serum levels of the enzyme (Mackenzie, 1982). Further histochemical investigation performed on patients with KHM demonstrates a positive staining for ß-glucuronidase activity within the keratinocytes, lamellar bodies, and the Langerhans cells as well. It has been suggested that possibly a large quantity of beta-glucuronidase enzyme is liberated from these various epidermal cells and migrates into the underlying dermal blood vessels thus causing the increase in its serum levels (Camisa and Rosanna, 1984). Furthermore, it has been postulated that the elevated levels of ß-glucuronidase found in the epidermis may actually play a direct role in the pathological process of the disease itself.

The processes of epidermal cell proliferation and metabolism are highly influenced by the plasma membrane glycoprotein receptors, as well as, by extracellular constituents containing most probably various polysaccharides (Noriega et al. 1993). In addition, hyaluronic acid has also been found to be synthesized by cultured human epidermal cells in vitro and may also be present within the epidermal intercellular spaces (Dingle et al. 1979). Studies have demonstrated that intercellular beta-glucuronidase may somehow degrade the plasma membrane glycoprotein receptors and their contents thereby altering the regulation of epidermal proliferation. It may further be postulated that the migration of ß-glucuronidase into the dermal tissues could also result in the alteration of dermal ground substance thus contributing to the development of psuedo-ainhum, a characteristic symptom of many patients suffering with KHM (Camisa and Rosanna, 1984).

The release of ß-glucuronidase from epidermal cells may be due to a variety of different factors such as leakage, secretion, or even the actual destruction of these cells. The lamellar body is the most likely candidate for the release of ß-glucuronidase enzyme (Yeshida, 1991). The lamellar body represents a modified lysosome, which functions to actively secrete its contents into the intercellular spaces. In addition, the lamellar body also contains various substances which comprise the major components of these epidermal intercellular spaces including glycoproteins, polysaccharides, and various acid hydrolases such as beta-glucuronidase and acid phosphatase.

Although ß-glucuronidase is found primarily in the lysosomes, it may play an important role along with the other glycosides in the lamellar bodies of the stratum corneum. The importance of glycosidases in the maturation of the stratum corneum has already been established and verified by previous studies using lectins for various carbohydrates. These studies have conclusively demonstrated that the carbohydrate (charged sugar) residues found in the stratum granulosum are completely eliminated within the stratum corneum. Thus, removal of these charged sugar groups would create a more hydrophobic environment between the keratinocyte intercellular spaces. Although these intercellular spaces already have a large lipid content, they in addition, also contain water due to these charged residues. The sugar removal further increases the nonpolar lipid content since polar glycosphingolipids are later converted to nonpolar lipids (Nemanic et al. 1988). While these sugar residues are present, the lamellar body network necessary for the effective barrier against water may not able to properly develop.

The success of synthetic retinoids in the treatment of KHM may further support the role ß-glucuronidase plays in the pathogenesis of this particular disease. Aromatic

retinoids have been reported to change epithelium from a predominantly keratinizing to a mucin-producing state. It may then be postulated that the effects of the retinoid treatment may compensate for the increased serum enzymatic activity by producing higher levels of polysaccharides (Albert et al. 1981).

Aromatic retinoids are certainly a step in the right direction in the treatment of Vohwinkel's Syndrome but hopefully, future research will provide these patients with a definite cure.

V. *Loricrin*:

Loricrin is a 26kD cationic protein rich in glycine, serine and cysteine residues. It is initially expressed in the stratum granulosum layer of the human epidermis. During the terminal differentiation process of the epidermis, the keratinocytes acquire a dense 15 nm thick layer of protein on the inner surface of the cellular membrane, which is known as the cornified cell envelope (CE). The deposition of various protein components, including loricrin, results in a gradual thickness of and rigidity of the CE. In addition, this highly resistant protein layer provides a vital barrier for the epidermis. Loricrin has now been established as the major structural component of this highly insoluble layer.

The cornified cell envelope is stabilized by many disulfide bonds and by the presence of N^{ε}-(γ-glutamyl) lysine isodipeptide crosslinks formed by the actions of epidermal transglutaminases. The protein loricrin constitutes as much as 70% of the overall mass of the CE contributing greatly to its stability and insolubility (Candi et al. 1995). The gene for loricrin is unique. Structurally, loricrin can be subdivided into discrete domains. There are three long glycine-serine-cysteine rich domains separated by glutamine rich sequences and bounded by lysine and glutamine rich amino and carboxy terminal end domains. Most probably these glutamine and lysine/glutamine domains serve as substrates for the transglutaminases and are involved in the crosslinking of these amino acid residues. The most striking feature of loricrin is its unique configuration of these specific residues (glycine-serine-cysteine) into three tandem quasi peptide repeats forming what are known as the glycine loop structures (Hohl, Mehrel et al. 1991). These

glycine loops provide flexibility to the cornified envelope and to the entire epidermis as well.

The assembly of the cornified envelope is thought to occur in a complex yet orderly fashion involving the sequential deposition of distinct protein components along with a gradual progression of envelope thickness and rigidity. The correct formation of the CE is thought to be essential for the formation of a normally functioning keratinized epidermis. The current model postulates that the initial step involves the early deposition of involucrin and other proteins that become attached to the lipid envelope to form a scaffold. In the second step, loricrin and other less abundant proteins are added to the initial scaffold on the cytoplasmic side of the cornified envelope (Steinert and Marekov, 1995). However, despite the abnormalities of the CE in palmoplantar keratodermas, such as Vohwinkel's Syndrome, little is known about the pathophysiological role it plays in these disorders. Recent studies have identified a defect in the gene encoding loricrin, the major constituent of the cornified envelope. The chromosomal localization of the loricrin gene was found to be in the position 1q21, mapped within the epidermal differentiation complex (EDC). In patients with Vohwinkel's Syndrome, sequencing of the loricrin gene revealed an insertion that shifts the translation frame of the C-terminal glycine and glutamine/lysine rich domains which impairs cornification (Ishida-Yamamoto and Iizuka, 1998). More specifically, an insertion of a glycine residue was found in an area of six normally occurring glycine residues (codons 230-231) of the loricrin gene (Maestrini et al. 1996). Consequently, the carboxyl-terminal 84 amino acids are replaced by highly charged missense sequences that override the endogenous termination codon extending the loricrin protein with an additional 22 amino acids (Korge et al. 1997). The

replacement of the fourth glycine rich domain and the C-terminal glutamine/lysine rich domain, which is thought to be involved in cross-linking, is likely to alter the function of the protein and to impair crosslinking by transglutaminases. This frameshift mutation causes a significant decrease in the flexibility of the CE by impairing and disrupting its ability to properly crosslink loricrin and other protein molecules.

Biopsies of patients with Vohwinkel's Syndrome clearly revealed an increased expression of loricrin distributed diffusely within the granular layers (Magnoldo et al. 1992). These findings indicate that loricrin is abnormally or less efficiently incorporated into the CE, and is found to accumulate within the granular layers. In addition, the CE of these patients was found to be abnormally thin and lucid in nature. The finding of a pathogenenic mutation in loricrin is the first implication of a defect in a structural gene of the cornified envelope in human palmoplantar disorders.

This study represents a part of a larger investigation to further understand the overall pathological process that defines KHM and all the factors that play a significant role in the manifestation of this particular disease. To date, we were able to isolate and identify specific characteristics that distinguish KHM skin from normal skin through both SEM and TEM studies. In addition, we were able to determine the quantitative levels of ß-glucuronidase activity in a KHM patient and compare these values to patients without KHM. Lastly, we are able to localize the loricrin protein through the use of immunogold labeling of the loricrin antibody. Immunoelectron microscopic analysis of the cornified envelope revealed the presence of loricrin, as well as, provided novel insights into the epidermal differentiation process.

Materials and Methods

I. *Scanning Electron Microscopy*:

A. *Materials*:

An adult male inbred mouse (BALB/cANTacfBR) obtained from Taconic Quality Laboratory Animals and Services for Research, a 3 mm punch, 70% ethanol solution, 2% glutaraldehyde in 0.2 M cacodylate buffer (pH 7.2), paraformaldehyde fixative (pH 7.2), 0.2 M cacodylate buffer, 2% osmium tetroxide in 0.2 M cacodylate buffer, 100% ethanol, liquid nitrogen, single edge razor, parafilm sleeves, ethanol dehydration series: 25%, 50%, 70%, 90%, 95% and 100% (twice), aluminum mounting stubs, double sticky tape and colloidal silver mounting media.

B. *Preparation of Reagents*:

0.2 M Cacodylate Buffer at pH 7.2: Cacodylate (dimethyl arsenic acid) buffer is the solution of choice in this study because of its specific ability to accurately preserve enzymatic activity. Furthermore, it is able to decrease unwanted artefacts in the specimen and in addition, it also possesses a high resistance to bacterial contamination (Hayat, 1981). The buffer was prepared according to the following protocol obtained in E.M. Hayat's Fixation for Electron Microscopy.

Solution A: (0.4 M)
21.4 g of sodium cacodylate [$Na(CH_3)_2AsO_2 \cdot 3\ H_20$]
250 mL distilled water

Solution B: (0.2 M)
9 mL of concentrated HCl (36-38%)
91 mL of distilled water

A physiological pH of exactly 7.2 was obtained by adding 8 mL of Solution B to

50 mL of Solution A and diluting to a total volume of 100 mL with distilled water.

2 % Glutaraldehyde in 0.2 M Cacodylate Buffer at pH 7.2 : Glutaraldehyde is a non-coagulant fixative that has a strong capacity to stabilize most proteins (Hayat, 1981). A commercially prepared 4% glutaraldehyde solution was diluted with 0.2 M cacodylate buffer solution at pH 7.2 (Postek et al. 1980).

Paraformaldehyde Fixative at pH 7.2: (Karnovsky's fixative) Paraformaldehyde is an extremely strong non- coagulative fixative that maintains cellular integrity and preserves the cellular contents and internal structures (Hayat, 1981). The paraformaldehyde solution was prepared as follows according to Karnovsky's procedure in E. M. Hayat's Fixation for Electron Microscopy.

20 mL of 10% paraformaldehyde in water
50 mL of 0.2 M cacodylate buffer at pH 7.2
10 mL of 25% stock glutaraldehyde solution
20 mL distilled water
1.0 N NaOH

In a fumed hood, 2 g of paraformaldehyde was dissolved in 20 mL distilled water by heating to 65°C with continuous stirring. Then a few drops of 1.0 N NaOH were slowly added until the solution became clear. The solution was cooled before use and the cacodylate buffer was added, as well as, the glutaraldehyde solution. Finally, 20 mL of distilled water was added and the pH was adjusted.

2 % Osmium Tetroxide in 0.2 M Cacodylate Buffer: Osmium tetroxide is a highly dangerous and volatile fixative. Its main mode of action is to cross link lipids or other

molecules at points of nonsaturation (Hayat, 1981). With extreme caution, under a fumed hood, a 1 g vial of osmium tetroxide (OsO_4) solution was added to a 50 mL of cacodylate buffer solution.

C. *Methods*:

The punch biopsy is the most basic of all biopsy techniques. It is performed with a circular cutting instrument known as a punch. The punch used for this specific project had a diameter of 3 mm. The skin samples used in this procedure were taken from the ear of an adult male mouse (type BALB/c). Three punches were taken per ear and the remainder of the ear was sectioned into small pieces. All tissue samples were immediately submerged in 70% ethanol directly after removal. Great care was taken during the procedure so as not to crush the tissue samples. The samples were then placed in 2% glutaraldehyde solution with 0.1 M cacodylate buffer at pH 7.2 for 10 minutes. The tissue samples were then transferred to the paraformaldehyde fixative and left overnight to insure proper fixation. The following day, the samples were removed from the paraformaldehyde fixative, washed in 0.2 M cacodylate buffer at pH 7.2 for 15 minutes. The post-fixation occurred in 2% osmium tetroxide in 0.2 M cacodylate buffer at pH 7.2 for 45 minutes. The samples were then rinsed in 0.2 M cacodylate buffer at pH 7.2 and then taken through an ethanol series: 25%, 50%, 70%, 90%, 95% and 100% (twice). At this point, half of the tissue samples were placed in 70% ethanol and reserved for freeze-fracture studies. The samples were then critical point dried, mounted on aluminum mounting stubs and sputter coated with 18 nm of vaporized gold. The precise method for freeze-fracture technique is outlined in detail below.

II. *Ethanol Cryofractography For SEM*:

Cryofracturing is a very useful technique in preparing small samples in which the fine details of internal structure are to be studied. Fixed and dehydrated samples are frozen in liquid nitrogen and are cut with a cooled razor blade. The blade does not actually cut the sample, but rather fractures it, thereby producing a very clean surface, free of many artefacts associated with simply cutting specimens at room temperature. The method usually works best when the sample is fractured after dehydration but prior to critical point drying. Cryofracturing is an easy technique, its only drawback is that precise control over the location of the fracture is difficult. Ethanol cryofractography followed by critical point drying provides a simple and rapid method for observing fine detail of biological structures in the SEM (Humphreys, 1974).

Methods: While still submerged in alcohol, the specimens were inserted into sleeves made from Parafilm and enclosed tightly. The sleeve was then held with a pair of fine point diamond- tipped tweezers and held in liquid nitrogen until sufficiently frozen. The sleeve was then placed on a pre-cooled flat metal surface and fractured with a pre-cooled single edge razor blade. The fractured specimen fragments were then submerged in a 70% ethanol solution for thawing. The specimens were then critical point dried using liquid CO_2, mounted on aluminum mounting stubs, and coated with a thin layer (18 nm) of vaporized gold.

III. *PELDRI II*: an alternative to critical point drying

Peldri II is a fluorocarbon solid at room temperature and is a liquid above 25°C. Cells or tissues are embedded in Peldri II by immersing them in the liquid form and allowing them to solidify. Once solidified, Peldri II will sublime with or without vacuum to dry biological tissues, without introducing any surface tension into the specimen. This alternative to critical point drying greatly enhanced and preserved all surface details.

Methods: All samples were stored in 100% ethanol until use. The Peldri II was warmed in a 35-40°C water bath for approximately 20 minutes until liquefied. The specimens were then submerged in a 1:1 mixture (50 mL ethanol: 50 mL Peldri II) for 1 hour. The samples were then submerged in a 100% solution of Peldri II for 1 hour. Afterwards, the specimens were placed on a warming plate to maintain a Peldri liquid state for 30 minutes. The samples were then cooled with ice at 25-30°C for approximately 25 minutes until the Peldri II solidified. The samples were then removed from the Peldri II and placed in a vacuum dessicator for 3 hours, until completely free of any moisture. The specimens were then mounted on an aluminum mounting stub with colloidal silver mounting media and coated with 18 nm of vaporized gold.

IV. *TRANSMISSION ELECTRON MICROSCOPY:*

A. *Materials*:

The skin samples used in this procedure were taken from the ear of an adult male mouse (type BALB/C). Three punches were taken per ear and the remainder of the ear was sectioned into smaller pieces. All tissue samples were immediately submerged in 70% ethanol directly after removal. Skin samples were obtained from both a KHM patient, as well as, a healthy patient using a 3 mm punchy biopsy, copper specimen grids used to mount the samples, 2% glutaraldehyde in 0.1 M cacodylate buffer (pH 7.4), 2 mM $CaCl_2$ (pH 7.4), a 0.1 M cacodylate buffer solution with 2 mM $MgCl_2$ (pH 7.4), 1% OsO_4 in 0.1 M cacodylate buffer (pH 7.4), ethanol dehydration series: 50%, 70%, 95% and 100% (twice), a 1:1 solution of ethanol and propylene oxide, propylene oxide, BEEM capsules and EMbed 812 filtration resin.

B. *Preparation of Reagents*:

Please refer to the previous section under SEM Studies.

C. *Methods*:

The skin samples used in this procedure were taken from the palmar skin of both a KHM patient, as well as, a healthy subject who was used as the control. The samples were obtained using a standard 3 mm punch and the procedure was performed by a certified dermatologist. The first samples (Sample A) obtained from both patients were dry samples. The second set of samples (Sample B) from both patients were obtained after soaking the palms in water for a full 20 minutes. All samples were immediately submerged in a 70% ethanol solution subsequent to their removal. Great care was taken during the procedure so as not to crush the tissue samples. The samples were then stored in a 2% glutaraldehyde

solution with 0.1 M cacodylate buffer at pH 7.4 overnight. The tissue samples were then fixed by immersion for 1 hour at room temperature in a 2% glutaraldehyde solution with 0.1 M cacodylate buffer at pH 7.4 containing 2.0 mM $CaCl_2$. The excess fixative solution was then removed by rinsing for 10 minutes in a 0.1 M cacodylate buffer solution containing 2.0 mM $MgCl_2$ at pH 7.4. Post-fixation of the samples was accomplished using a 1% OsO_4 in a 0.1 M cacodylate buffer at pH 7.4 for 1 hour. The excess fixative is then washed off in a 0.1 M cacodylate buffer at pH 7.4 for 10 minutes. The samples were then taken through a graded ethanol series: 50% (15 minutes), 70% (20 minutes), 95% (30 minutes) and lastly for 100 % (twice at 30 minutes each time). The samples were placed in a 1:1 ethanol-propylene oxide solution for 30 minutes. Next, a resin mixture is then substituted for the ethanol through an intermediate which is miscible in both solutions. The intermediate solution we used was propylene oxide. The samples were immersed for 30 minutes in propylene oxide, this was done twice. The individual tissue samples were then placed in BEEM capsules filled with EMbed 812 resin at room temperature in the following manner: a 1:3 mixture of EMbed 812 to propylene oxide for 30 minutes followed by a 1:1 mixture for 1 hour, then a 3:1 mixture of EMbed 812 to propylene oxide for 1 hour followed by a 100% EMbed 812 solution for 1 hour. Lastly, the samples were placed overnight in a 70° C oven immersed in EMbed 812. Following polymerization of the tissue samples, the resin tissue blocks were then trimmed and sectioned using an Reichert-Jung Ultracut E Ultra Microtome. The sections were sliced 0.5μm thick. Lastly, the samples were then mounted on a copper specimen grid.

V. *Quantitative Determination of ß-Glucuronidase*:

A. *Materials*:

A DU Series 60 Spectrophotometer, standard serological pipets (1, 5, 10 mL), a 25 mL graduated cylinder, Erlenmeyer flask, standard test tubes, dialysis tubing, dialysis sacks and a 56°C water bath.

B. *Reagents Used*:

Acetate Buffer Solution: 0.2 mol/L sodium acetate (pH 4.5 at 25°C).

Phenolphthalein Glucuronic (PG) Acid Solution: 0.03 mol/L phenolphthalein mono-ß-glucuronic acid (pH 4.5 at 25°C).

2-Amino-2-Methyl-1-Propanol (AMP) Buffer: 0.1 mol/L AMP (pH 11) and 0.2% sodium lauryl sulfate.

Phenolphthalein Standard Solution: 1 mg/mL phenolphthalein in ethanol.

C. *Methods*: (serum assay)

Approximately 5 mL of blood was obtained from an inbred adult male mouse (type BALB/c). The blood was then centrifuged for 15 minutes and the serum was recovered. This assay was performed on five different samples. Three test tubes were used; one labeled Serum Blank (SB), the other labeled Test (T), and the third labeled Reagent Blank (RB). The reagents were added as follows:

COMPONENT	RB (mL)	SB (mL)	T (mL)
Acetate Buffer Solution	0.6	0.6	0.6
PG Acid Solution	0.2	---	0.2
Water	0.2	0.2	----
Serum	---	0.2	0.2

Each tube was then swirled to ensure proper mixing had occurred. The tubes were then placed in a 56°C water bath and incubated for exactly one hour. Immediately following the incubation, 5.0 mL AMP Buffer was added to each test tube. The tube was then swirled to properly blend all of the ingredients. The absorbence of each tube was read at 550 nm using a spectrophotometer. A test tube filled with water was use as a reference.

D. *Calibration*: for serum assay

An individual calibration curve was required to properly assess the obtained data. Diluents for phenolphthalein standards were prepared.

Diluent **S** for serum calibration curve contained the following:

3.6 mL Acetate buffer solution

2.4 mL water

30.0 mL AMP buffer

A diluted phenolphthalein solution (40 μg/mL) was prepared by combining 0.2 mL Phenolphthalein Standard solution with 4.8 mL of Diluent S. The calibration solutions were prepared as follows:

TUBE #	Diluted pH. soln. (mL)	Diluent S (mL)	pH. conc. (ug/mL)
1	0.3	5.7	2.0
2	0.6	5.4	4.0
3	0.9	5.1	6.0
4	1.2	4.8	8.0

The absorbence of tubes 1-4 were read using a spectrophotometer at 550 nm using water as a reference.

E. *Urine Dialysis*:

Urine samples were obtained from a 25 year old male KHM patient, a 25 year old healthy male (control #1), and a 25 year old healthy female (control #2). First, the dialysis tubing was soaked in water for 5 minutes to increase its flexibility. Then, 25 mL of collected urine sample was centrifuged for 15 minutes. Next, 15 mL of the centrifuged urine was poured into a dialysis sack and secured tightly on both ends. The sack was then immersed in a 250 mL Erlenmeyer flask filled with cold water. The length of the softened tubing was then fastened to the water tap and the water flow was adjusted to about 25-50 mL per minute. The other end of the rubber tubing was inserted into the bottom of the flask and the flask was placed in the sink. The dialysis continued for 2 hours, after which the content of the sack was carefully measured. The volume (V) was recorded in mL and a Dialysis Dilution Factor (DDF) was calculated using the following formula: $DDF = {}^{V}/_{15}$.

F. *Assay of Dialyzed Urine*:

Three test tubes were used, one labeled Urine Blank (UB), a second labeled Reagent Blank (RB) and the other Test (T). The reagents were added as follows:

COMPONENT	RB (mL)	UB (mL)	T (mL)
Acetate Buffer Solution	0.3	0.3	0.3
PG Acid Solution	0.2	----	0.2
Water	0.5	0.2	----
Dialyzed Urine	----	0.5	0.5

The test tubes were mixed by swirling and then placed in a 56°C water bath to incubate for exactly 1 hour. Immediately following the incubation, 5.0 mL AMP Buffer was added to

each test tube. The tubes were swirled to ensure proper mixing. The absorbence of each tube was read at 550 nm using the DU Series 60 Spectrophotometer and water as the reference.

G. *Calibration*: for urine assay

An individual calibration curve was required to properly assess the obtained data. Diluents for phenolphthalein standards were prepared.

Diluent **U** for serum calibration curve contained the following:

1.8 mL Acetate buffer solution

4.2 mL water

30.0 mL AMP buffer

A diluted phenolphthalein solution (40 µg/mL) was prepared by combining 0.2 mL of Phenolphthalein Standard solution with 4.8 mL of Diluent U. The calibration solutions were prepared as follow:

TUBE #	Diluted pH. soln. (mL)	Diluent S (mL)	pH. conc. (µg/mL)
1	0.3	5.7	2.0
2	0.6	5.4	4.0
3	0.9	5.1	6.0
4	1.2	4.8	8.0

The absorbence of tubes 1-4 were read using a DU Series 60 spectrophotometer at 550 nm with water as the reference.

VI. *Loricrin*:

The use of colloidal gold with silver enhancement in conjunction with a low temperature embedding immunolabeling technique allows for the localization of antigens within the skin. This specific method allows for the best structural preservation and the greatest intensity of immunolabeling. Furthermore, immunocytochemical localization of antigenic sites on the surfaces of thin sections permits direct access to intracellular antigens without limitation by the plasma membrane or internal membranes of the cell. The results are an increase in the sensitivity of detection. Lowicryl K11M was introduced as a low temperature embedding medium particularly well suited for applications in immunoelectron microscopy. This resin is composed of polar acrylates and methylacrylates and has the ability to infiltrate tissues at very low temperatures (Shimuzu et al. 1992). Lowicryl's other characteristics also include high resolution of structural images while retaining a high degree of preservation of protein antigenicity.

Biopsy skin samples were obtained from the patient and cut into small pieces (<2 mm). The samples were then washed in PBS (phosphate buffered saline at pH 7.4) for 2 hours at 4° C and then fixed with 1% glutaraldehyde and 0.2% picric acid in PBS at pH 7.4 for 3 hours at room temperature. The tissue samples were then washed in PBS for 1 hour at 4° C and rinsed 2 times in 0.25 M citrate buffer at pH 7.4. The samples were then mounted on 200 mesh nickel grids and incubated with primary antibody 1:25 (a rabbit polyclonal antibody raised against a mouse loricrin N-terminal peptide) diluted in 1% NGS (normal goat serum), 1% BSA (bovine serum albumin), 0.1% gelatin, 0.02% sodium azide in PBS overnight at 4° C.

The samples were then washed in PBS for 6 hours at 4° C and the incubated with secondary antibody comprised of 5 nm immunogold conjugated to secondary goat anti-rabbit antibody diluted (1:3) in 1% NGS, 1% BSA, 0.1% gelatin, 0.02% sodium azide, 0.9% NaCl and 20 nm Tris-HCl buffer at pH 8.2 overnight at 4° C. The samples were again washed in PBS for 2 hours at room temperature. This double-labeling technique ensures the proper localization of the loricrin antigenic sites.

The silver staining was performed for approximately 7-9 minutes to enhance visualization at room temperature using a silver enhancement kit solution diluted (1:1) with distilled water and the reaction was stopped by immersing the specimens in 0.25M citrate buffer at pH 7.4. The tissue was then dehydrated through an ethanol series (35%, 50%, 75%, 90%,100%).

Lastly, uranyl acetate en bloc staining and embedding in K11M resin was performed. After tissue preparation, the dehydrated samples were then transferred into a 1:1 mixture of ethanol:lowicryl for 1 hour, a 1:2 mixture for another hour and then finally into undiluted 100% lowicryl overnight. The samples were then transferred into fresh lowicryl for 5 hours and then placed into BEEM capsules and polymerized at 4° C under UV lighting for 2 days. The final step of polymerization is completed under UV lighting at room temperature. The samples were the cut into superficial semi-thin sections, as well as, ultra-thin sections and stained with 5% uranyl acetate for 10 minutes and lead citrate for 10-20 seconds for heightened contrast (Ishida-Yamamoto et al. 1996).

Great strides have been made in the last decade in the ease and reliability of immunological labeling for electron microscopy. This technique can efficiently permit

the localization, quantification and quantitation of specific biochemical entities at a resolution unattainable by other means.

RESULTS

I. Quantitative Determination of ß-Glucuronidase Enzyme:

ß-glucuronidase (ß-D-glucuronoside glucuronosohydrolase) is a tetrameric glycoprotein composed of four identical subunits. The monomers are synthesized as precursors of approximately M_r = 75,000-82,000 and are proteolytically processed at the carboxy-terminus either prior to or soon after reaching the lysosome (Noriega et al. 1993). ß-glucuronidase is predominantly localized within the lysosome. The enzyme acts within the acidic environment of the lysosome as an exoglycosidase to remove terminal ß-glucuronic acid residues from the non-reducing end of glycosaminoglycans (GAGS) and other glycoconjugates. Mammalian ß-glucuronidase has a broad pH optimum ranging between 3.8-5.0 (Noriega et al. 1993).

ß-glucuronidase enzyme specifically catalyzes biochemical reactions involving the transfer of glucuronyl radicals to various acceptor alcohols (Noriega et al. 1993). The enzyme is highly abundant in the liver, spleen, pancreas, and other vital tissues including the epidermis. It has been suggested that the activity of this particular enzyme reflects the degree of cellular proliferation taking place in a tissue or organ (Rutenberg et al. 1973). An increase in its circulating concentration provides great clinical significance in many types of pathological processes, including KHM. Urinary excretion of the enzyme is also considered to provide valuable diagnostic information. Elevated levels of enzymatic activity are routinely encountered in patients diagnosed with Vohwinkel's Syndrome. Thus, a definitive relationship between ß-glucuronidase and proliferative activity does indeed exist.

The following illustration depicts the partial organic structure of the active site on the ß-glucuronidase enzyme:

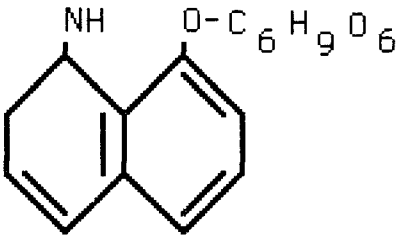

The enzyme itself has been assayed by methods involving the hydrolysis of various types of glucuronides. In 1967, Fishman and his colleagues, introduced a simplified procedure employing phenolphthalein glucuronic acid as the substrate for ß-glucuronidase activity (Fishman et al. 1967). According to this technique, the complex is first cleaved by ß-glucuronidase, releasing phenolphthalein which is then determined colorimetrically via a spectrophotometer.

The assay technique employed in our study is similar to the one proposed by Fishman and his co-workers. According to this particular procedure, ß-glucuronidase acts on phenolphthalein mono-ß-glucuronic acid to liberate free phenolphthalein. Phenolphthalein glucuronide ($C_{20}H_{14}O_4$) is an H^+ ion indicator dye (McClung, 1967). The intensity of the resulting red color in alkali was measured at 550 nm using a spectrophotometer and is proportional to its enzymatic activity. This color change is due to the dissociation of the OH-group (McClung, 1967). [The following figure illustrates the specific reaction that occurs]. The ß-glucuronidase enzyme activity was measured by both serum and urine assays.

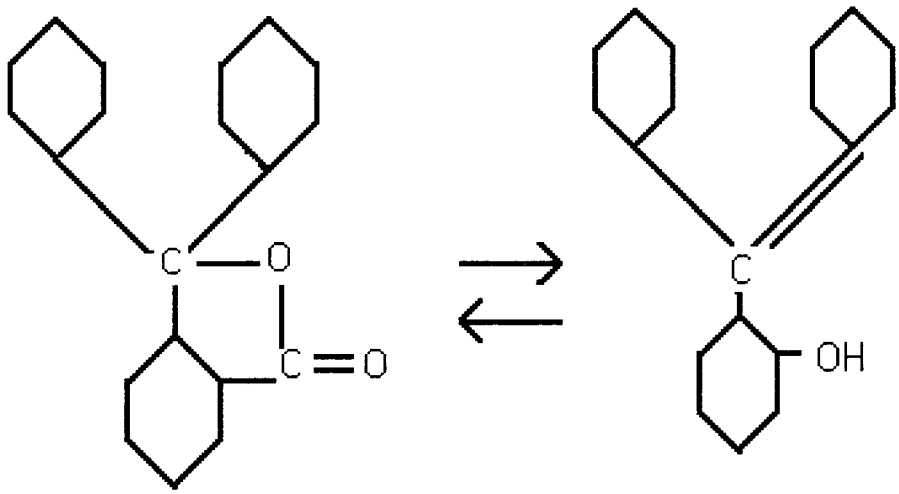

(Colorless phenolphthalein)

The procedure for the quantitative determination of ß-glucuronidase in serum was performed on five adult male inbred mice (BALB/cANTacfBR) obtained from Taconic Quality Laboratory Animals and Services for Research. Three test tubes were used; one labeled SERUM BLANK (SB), the other labeled TEST (T), and the third labeled REAGENT BLANK (RB). The calculations were based on determining the corrected absorbence (A) of TEST (T) as follows:

$$\text{Corrected } A = A_T - [A_{SB} + A_{RB}]$$

Using this Corrected A value, the phenolphthalein concentration (µg/mL) was determined from the Serum Calibration Curve found on the following page. The serum ß-glucuronidase activity was then calculated in Modified Sigma Units/mL using the following formula:

Serum ß-glucuronidase (Modified Sigma Units/mL)

= Phenolphthalein Concentration (µg/mL) x 30.

Where the unit definition is equal to one Modified Sigma Unit of ß-glucuronidase activity which will liberate 1µg of phenolphthalein from phenolphthalein glucuronic acid per hour at 56 °C.

SERUM CALIBRATION CURVE:

The absorbence of each tube was read at 550 nm using the DU Series 60 Spectrophotometer and water as the reference.

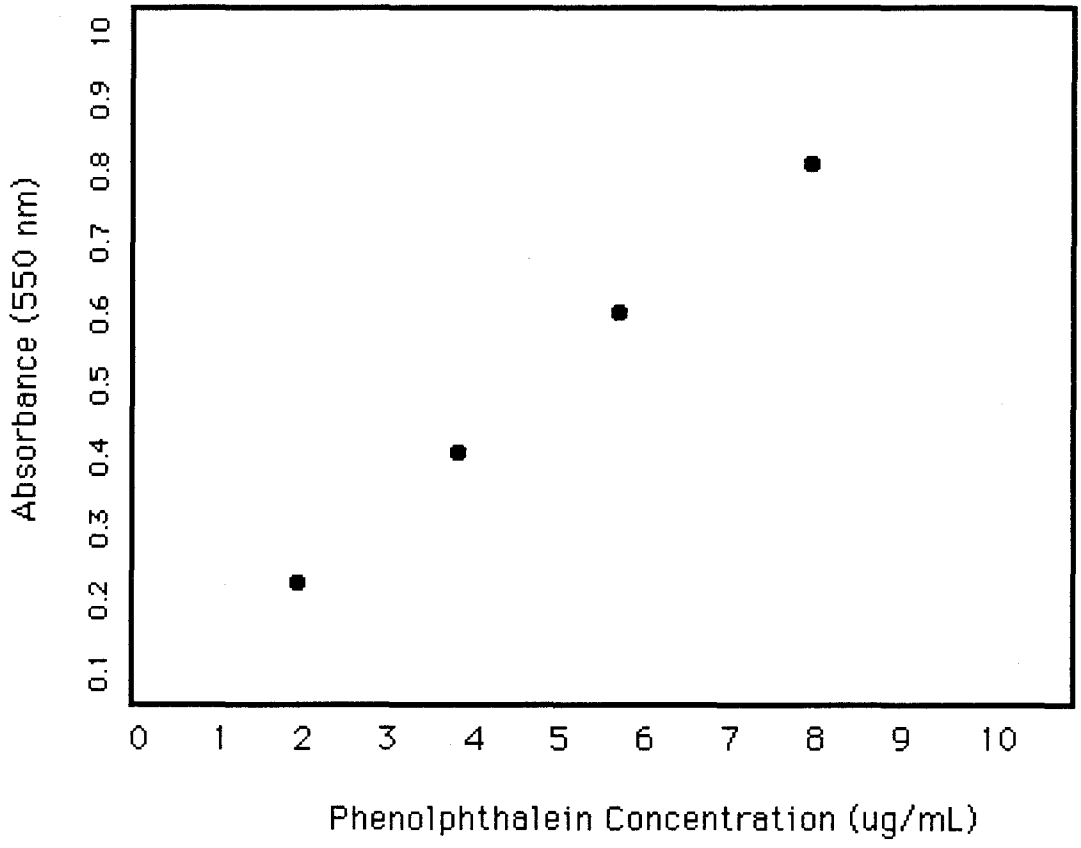

Calibration Solutions:

Tube 1: 0.223

Tube 2: 0.411

Tube 3: 0.621

Tube 4: 0.812

The results for the quantitative determination of ß-glucuronidase activity in serum are as follows:

Mouse #1:

The absorbencies obtained were as follows:

$T_1 = 0.159$

$SB_1 = 0.074$

$RB_1 = 0.026$

$$\text{Corrected A} = A_{T_1} - [A_{SB_1} + A_{RB_1}]$$

$$A_1 = 0.159 - (0.074 + 0.026)$$

$$A_1 = 0.059$$

The phenolphthalein concentration (µg/mL) was derived from the serum calibration curve and used to calculate ß-glucuronidase activity as follows:

Serum ß-glucuronidase (Modified Sigma Units/mL)

= Phenolphthalein Concentration (µg/mL) x 30

From the serum calibration curve, the Corrected A is equivalent to a phenolphthalein concentration of 0.60 µg/mL. Thus, for Mouse #1, the serum ß-glucuronidase (Modified Sigma Units/mL) = 0.60 x 30 = 18.

Mouse #2:

The absorbencies obtained were as follows:

$T_2 = 0.153$

$SB_2 = 0.072$

$RB_2 = 0.024$

Corrected $A = A_{T_2} - [A_{SB_2} + A_{RB_2}]$

$A_2 = 0.153 - (0.072 + 0.024)$

$A_2 = 0.057$

The phenolphthalein concentration (µg/mL) was derived from the serum calibration curve and used to calculate ß-glucuronidase activity as follows:

Serum ß-glucuronidase (Modified Sigma Units/mL)

= Phenolphthalein Concentration (µg/mL) x 30

From the serum calibration curve, the Corrected A is equivalent to a phenolphthalein concentration of 0.60 µg/mL. Thus, for Mouse #2, the serum ß-glucuronidase (Modified Sigma Units/mL) = 0.60 x 30 = 18.

Mouse #3:

The absorbencies obtained were as follows:

$T_3 = 0.189$

$SB_3 = 0.083$

$RB_3 = 0.046$

Corrected $A = A_{T_3} - [A_{SB_3} + A_{RB_3}]$

$A_3 = 0.189 - (0.083 + 0.046)$

$A_3 = 0.060$

The phenolphthalein concentration (μg/mL) was derived from the serum calibration curve and used to calculate ß-glucuronidase activity as follows:

Serum ß-glucuronidase (Modified Sigma Units/mL)

= Phenolphthalein Concentration (μg/mL) x 30

From the serum calibration curve, the Corrected A is equivalent to a phenolphthalein concentration of 0.60 μg/mL. Thus, for Mouse #3, the serum ß-glucuronidase (Modified Sigma Units/mL) = 0.60 x 30 = 18.

Mouse #4:

The absorbencies obtained were as follows:

$T_4 = 0.162$

$SB_4 = 0.076$

$RB_4 = 0.028$

Corrected $A = A_{T_4} - [A_{SB_4} + A_{RB_4}]$

$A_4 = 0.162 - (0.076 + 0.028)$

$A_4 = 0.058$

The phenolphthalein concentration (µg/mL) was derived from the serum calibration curve and used to calculate ß-glucuronidase activity as follows:

Serum ß-glucuronidase (Modified Sigma Units/mL)

= Phenolphthalein Concentration (µg/mL) x 30

From the serum calibration curve, the Corrected A is equivalent to a phenolphthalein concentration of 0.60 µg/mL. Thus, for Mouse #4, the serum ß-glucuronidase (Modified Sigma Units/mL) = 0.60 x 30 = 18.

Mouse #5:

The absorbencies obtained were as follows:

$T_5 = 0.187$

$SB_5 = 0.091$

$RB_5 = 0.037$

Corrected $A = A_{T_5} - [A_{SB_5} + A_{RB_5}]$

$A_5 = 0.187 - (0.091 + 0.037)$

$A_5 = 0.059$

The phenolphthalein concentration (µg/mL) was derived from the serum calibration curve and used to calculate ß-glucuronidase activity as follows:

Serum ß-glucuronidase (Modified Sigma Units/mL)

= Phenolphthalein Concentration (µg/mL) x 30

From the serum calibration curve, the Corrected A is equivalent to a phenolphthalein concentration of 0.60 µg/mL. Thus, for Mouse #5, the serum ß-glucuronidase (Modified Sigma Units/mL) = 0.60 x 30 = 18.

The results obtained from the serum assay of ß-glucuronidase indicates that all five adult male mice tested revealed the exact same level of enzymatic activity when measured in Modified Sigma Units/mL. Since ß-glucuronidase is found virtually in all mammalian tissues, it was quite easily detectable within mouse skin. Previous studies have indicated that the mouse epidermis, as a source of ß-glucuronidase activity, has been estimated to constitute as much as 3% of the total protein value (Goldbarg et al. 1975). The specific assay we used to determine ß-glucuronidase activity, which was supplied by Sigma Diagnostics Inc., and gave an estimated account of the enzyme's activity using the concentration of phenolphthalein which was determined colorimetrically by a spectrophotometer. The fact that the same results were obtained using five different mice while performing five different and separate assays indicates that the quantitative levels of mouse serum ß-glucuronidase is equivalent to 18 Modified Sigma Units/mL in this specific study. Thus, we were able to conclude that the level of ß-glucuronidase activity in the serum is quite stable for the particular mice (BALB/cANTacfBR) used in our study. In addition, this study allows for a high degree of reliability (reproducibility or repeatability) of our results.

The procedure for the quantitative determination of ß-glucuronidase in urine was performed on five different healthy control females and five different healthy control males all between the ages of 24-26 years. The assay was also performed five different times on a 25 year old adult male with KHM (Vohwinkel's Syndrome). Three test tubes were used; one labeled Urine Blank (UB), the other labeled Test (T), and the third labeled Reagent Blank (RB). The calculations were based on determining the corrected absorbence (A) of Test (T) as follows:

$$\text{Corrected } A = A_T - [A_{UB} + A_{RB}]$$

Using this Corrected A value, the phenolphthalein concentration (µg/mL) was determined from the Urine Calibration Curve found on the following page. The urine ß-glucuronidase activity was then calculated in Modified Sigma Units/mL using the following formula:

Urine ß-glucuronidase (Modified Sigma Units/mL)

= Phenolphthalein Concentration (µg/mL) x DDF x 12.

Where DDF (Dialysis Dilution Factor) = $\frac{\text{Volume (mL)}}{15}$

Where the unit definition is equal to one Modified Sigma Unit of ß-glucuronidase activity which will liberate 1µg of phenolphthalein from phenolphthalein glucuronic acid per hour at 56 °C.

URINE CALIBRATION CURVE:

The absorbence of each tube was read at 550 nm using the DU Series 60 Spectrophotometer and water as the reference.

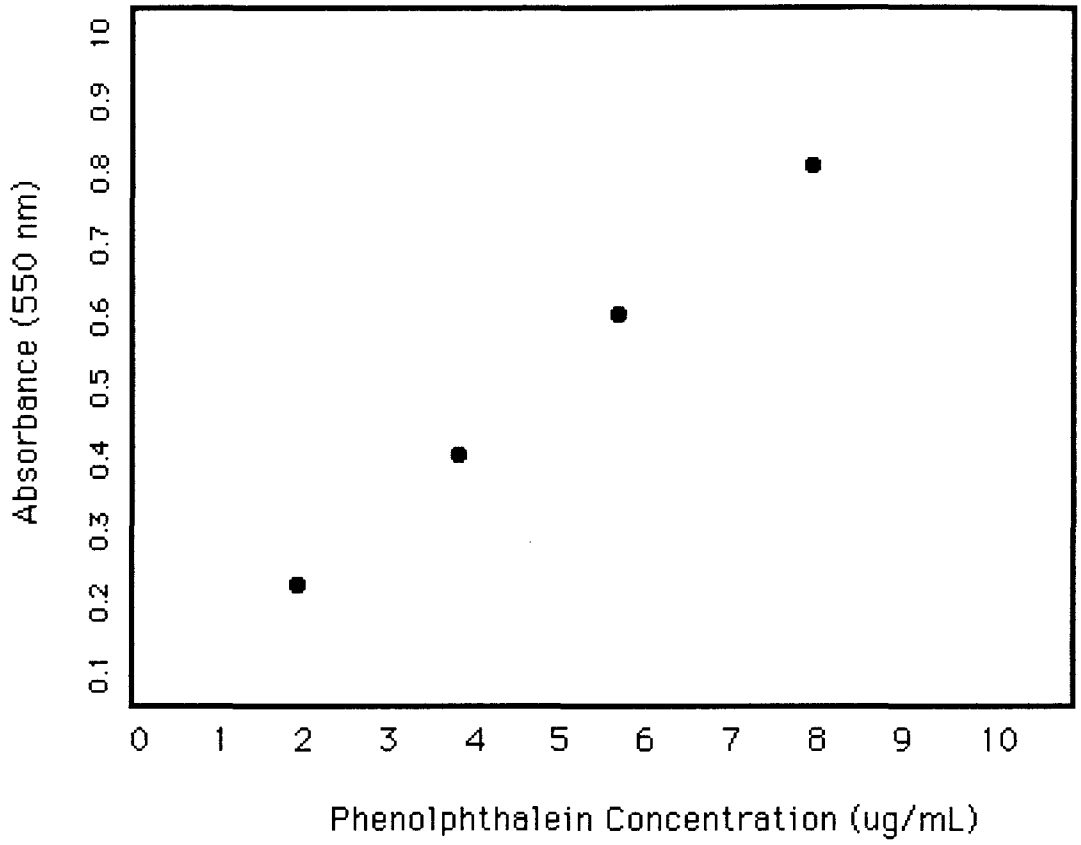

Calibration Solutions:

Tube 1: 0.216

Tube 2: 0.403

Tube 3: 0.614

Tube 4: 0.823

The results for the quantitative determination of ß-glucuronidase enzyme in adult control female urine samples are as follows:

Control Female #1:

The absorbencies obtained were as follows:

$T_1 = 0.150$

$UB_1 = 0.012$

$RB_1 = 0.036$

$$\text{Corrected A} = A_{T_1} - [A_{UB_1} + A_{RB_1}]$$

$$A_1 = 0.150 - (0.012 + 0.036)$$

$$A_1 = 0.102$$

$$\text{DDF} = \frac{19.5}{15} = 1.30 \qquad \text{Where V (mL)} = 19.5.$$

The phenolphthalein concentration (µg/mL) was derived from the urine calibration curve and used to calculate ß-glucuronidase activity as follows:

Urine ß-glucuronidase (Modified Sigma Units/mL)

= Phenolphthalein Concentration (µg/mL) x DDF x 12.

From the urine calibration curve, the Corrected A is equivalent to a phenolphthalein concentration of 1.00 µg/mL. Thus, for Female #1, the urine ß-glucuronidase (Modified Sigma Units/mL) = 1.00 x 1.30 x 12 = 15.6.

Control Female #2:

The absorbencies obtained were as follows:

$T_2 = 0.146$

$UB_2 = 0.011$

$RB_2 = 0.037$

Corrected $A = A_{T_2} - [A_{UB_2} + A_{RB_2}]$

$A_2 = 0.146 - (0.011 + 0.037)$

$A_2 = 0.102$

$DDF = \frac{18.0}{15} = 1.20$ Where V (mL) = 18.0.

The phenolphthalein concentration (µg/mL) was derived from the urine calibration curve and used to calculate ß-glucuronidase activity as follows:

Urine ß-glucuronidase (Modified Sigma Units/mL)

= Phenolphthalein Concentration (µg/mL) x DDF x 12.

From the urine calibration curve, the Corrected A is equivalent to a phenolphthalein concentration of 1.00 µg/mL. Thus, for Female #2, the urine ß-glucuronidase (Modified Sigma Units/mL) = 1.00 x 1.20 x 12 = 14.4.

Control Female #3:

The absorbencies obtained were as follows:

$T_3 = 0.152$

$UB_3 = 0.010$

$RB_3 = 0.034$

Corrected $A = A_{T_3} - [A_{UB_3} + A_{RB_3}]$

$A_3 = 0.152 - (0.010 + 0.034)$

$A_3 = 0.108$

$DDF = \frac{18.6}{15} = 1.24$ Where V (mL) = 18.6.

The phenolphthalein concentration (µg/mL) was derived from the urine calibration curve and used to calculate ß-glucuronidase activity as follows:

Urine ß-glucuronidase (Modified Sigma Units/mL)

= Phenolphthalein Concentration (µg/mL) x DDF x 12.

From the urine calibration curve, the Corrected A is equivalent to a phenolphthalein concentration of 1.05 µg/mL. Thus, for Female #3, the urine ß-glucuronidase (Modified Sigma Units/mL) = 1.05 x 1.24 x 12 = 15.6.

Control Female #4:

The absorbencies obtained were as follows:

$T_4 = 0.154$

$UB_4 = 0.014$

$RB_4 = 0.039$

Corrected $A = A_{T_4} - [A_{UB_4} + A_{RB_4}]$

$A_4 = 0.154 - (0.014 + 0.039)$

$A_4 = 0.101$

$DDF = \frac{19.3}{15} = 1.29$ Where V (mL) = 19.3.

The phenolphthalein concentration (µg/mL) was derived from the urine calibration curve and used to calculate ß-glucuronidase activity as follows:

Urine ß-glucuronidase (Modified Sigma Units/mL)

= Phenolphthalein Concentration (µg/mL) x DDF x 12.

From the urine calibration curve, the Corrected A is equivalent to a phenolphthalein concentration of 1.00 µg/mL. Thus, for Female #4, the urine ß-glucuronidase (Modified Sigma Units/mL) = 1.00 x 1.29 x 12 = 15.5.

Control Female #5:

The absorbencies obtained were as follows:

$T_5 = 0.148$

$UB_5 = 0.009$

$RB_5 = 0.034$

$$\text{Corrected A} = A_{T_5} - [A_{UB_5} + A_{RB_5}]$$

$$A_5 = 0.148 - (0.009 + 0.034)$$

$$A_5 = 0.105$$

$$\text{DDF} = \frac{18.2}{15} = 1.21$$ Where V (mL) = 18.2.

The phenolphthalein concentration (µg/mL) was derived from the urine calibration curve and used to calculate ß-glucuronidase activity as follows:

Urine ß-glucuronidase (Modified Sigma Units/mL)

= Phenolphthalein Concentration (µg/mL) x DDF x 12.

From the urine calibration curve, the Corrected A is equivalent to a phenolphthalein concentration of 1.05 µg/mL. Thus, for Female #5, the urine ß-glucuronidase (Modified Sigma Units/mL) = 1.05 x 1.21 x 12 = 15.2.

The results for the quantitative determination of ß-glucuronidase enzyme in adult control male urine samples are as follows:

Control Male #1:

The absorbencies obtained were as follows:

$T_1 = 0.183$

$UB_1 = 0.075$

$RB_1 = 0.022$

$$\text{Corrected A} = A_{T_1} - [A_{UB_1} + A_{RB_1}]$$

$$A_1 = 0.183 - (0.075 + 0.022)$$

$$A_1 = 0.086$$

$$\text{DDF} = \frac{22.0}{15} = 1.50 \qquad \text{Where V (mL)} = 22.0.$$

The phenolphthalein concentration (µg/mL) was derived from the urine calibration curve and used to calculate ß-glucuronidase activity as follows:

Urine ß-glucuronidase (Modified Sigma Units/mL)

= Phenolphthalein Concentration (µg/mL) x DDF x 12.

From the urine calibration curve, the Corrected A is equivalent to a phenolphthalein concentration of 0.80 µg/mL. Thus, for Control Male #1, the urine ß-glucuronidase (Modified Sigma Units/mL) = 0.80 x 1.50 x 12 = 14.4.

Control Male #2:

The absorbencies obtained were as follows:

$T_2 = 0.186$

$UB_2 = 0.078$

$RB_2 = 0.024$

Corrected $A = A_{T_2} - [A_{UB_2} + A_{RB_2}]$

$A_2 = 0.186 - (0.078 + 0.024)$

$A_2 = 0.084$

$DDF = \frac{23.5}{15} = 1.60$ Where V (mL) = 23.5.

The phenolphthalein concentration (µg/mL) was derived from the urine calibration curve and used to calculate ß-glucuronidase activity as follows:

Urine ß-glucuronidase (Modified Sigma Units/mL)

= Phenolphthalein Concentration (µg/mL) x DDF x 12.

From the urine calibration curve, the Corrected A is equivalent to a phenolphthalein concentration of 0.80 µg/mL. Thus, for Control Male #2, the urine ß-glucuronidase (Modified Sigma Units/mL) = 0.80 x 1.60 x 12 = 15.4.

Control Male #3:

The absorbencies obtained were as follows:

$T_3 = 0.180$

$UB_3 = 0.073$

$RB_3 = 0.021$

Corrected $A = A_{T_3} - [A_{UB_3} + A_{RB_3}]$

$A_3 = 0.180 - (0.073 + 0.021)$

$A_3 = 0.086$

$DDF = \frac{21.7}{15} = 1.50$ Where V (mL) = 21.7.

The phenolphthalein concentration (µg/mL) was derived from the urine calibration curve and used to calculate ß-glucuronidase activity as follows:

Urine ß-glucuronidase (Modified Sigma Units/mL)

= Phenolphthalein Concentration (µg/mL) x DDF x 12.

From the urine calibration curve, the Corrected A is equivalent to a phenolphthalein concentration of 0.80 µg/mL. Thus, for Control Male #3, the urine ß-glucuronidase (Modified Sigma Units/mL) = 0.80 x 1.50 x 12 = 14.4.

Control Male #4:

The absorbencies obtained were as follows:

$T_4 = 0.183$

$UB_4 = 0.060$

$RB_4 = 0.020$

Corrected $A = A_{T_4} - [A_{UB_4} + A_{RB_4}]$

$A_4 = 0.183 - (0.060 + 0.020)$

$A_4 = 0.083$

$DDF = \frac{23.8}{15} = 1.60$ Where V (mL) = 23.8.

The phenolphthalein concentration (µg/mL) was derived from the urine calibration curve and used to calculate ß-glucuronidase activity as follows:

Urine ß-glucuronidase (Modified Sigma Units/mL)

= Phenolphthalein Concentration (µg/mL) x DDF x 12.

From the urine calibration curve, the Corrected A is equivalent to a phenolphthalein concentration of 0.80 µg/mL. Thus, for Control Male #4, the urine ß-glucuronidase (Modified Sigma Units/mL) = 0.80 x 1.60 x 12 = 15.4.

Control Male #5:

The absorbencies obtained were as follows:

$T_5 = 0.181$

$UB_5 = 0.062$

$RB_5 = 0.018$

Corrected $A = A_{T_5} - [A_{UB_5} + A_{RB_5}]$

$A_5 = 0.181 - (0.062 + 0.018)$

$A_5 = 0.081$

$DDF = \frac{22.4}{15} = 1.50$ Where V (mL) = 22.4.

The phenolphthalein concentration (μg/mL) was derived from the urine calibration curve and used to calculate ß-glucuronidase activity as follows:

Urine ß-glucuronidase (Modified Sigma Units/mL)

= Phenolphthalein Concentration (μg/mL) x DDF x 12.

From the urine calibration curve, the Corrected A is equivalent to a phenolphthalein concentration of 0.80 μg/mL. Thus, for Control Male #5, the urine ß-glucuronidase (Modified Sigma Units/mL) = 0.80 x 1.50 x 12 = 14.4.

The results for the quantitative determination of ß-glucuronidase enzyme in an adult KHM male urine samples are as follows:

KHM Male #1:

The absorbencies obtained were as follows:

$T_1 = 0.141$

$UB_1 = 0.014$

$RB_1 = 0.013$

Corrected $A = A_{T_1} - [A_{UB_1} + A_{RB_1}]$

$A_1 = 0.141 - (0.014 + 0.013)$

$A_1 = 0.114$

$DDF = \frac{29.4}{15} = 1.96$ Where V (mL) = 29.4.

The phenolphthalein concentration (µg/mL) was derived from the urine calibration curve and used to calculate ß-glucuronidase activity as follows:

Urine ß-glucuronidase (Modified Sigma Units/mL)

= Phenolphthalein Concentration (µg/mL) x DDF x 12.

From the urine calibration curve, the Corrected A is equivalent to a phenolphthalein concentration of 1.50 µg/mL. Thus, for KHM Male #1, the urine ß-glucuronidase (Modified Sigma Units/mL) = 1.50 x 1.96 x 12 = 35.3.

KHM Male #2:

The absorbencies obtained were as follows:

$T_2 = 0.139$

$UB_2 = 0.012$

$RB_2 = 0.012$

Corrected $A = A_{T_2} - [A_{UB_2} + A_{RB_2}]$

$A_2 = 0.139 - (0.012 + 0.012)$

$A_2 = 0.115$

$DDF = \frac{28.9}{15} = 1.93$ Where V (mL) = 28.9.

The phenolphthalein concentration (µg/mL) was derived from the urine calibration curve and used to calculate ß-glucuronidase activity as follows:

Urine ß-glucuronidase (Modified Sigma Units/mL)

= Phenolphthalein Concentration (µg/mL) x DDF x 12.

From the urine calibration curve, the Corrected A is equivalent to a phenolphthalein concentration of 1.50 µg/mL. Thus, for KHM Male #2, the urine ß-glucuronidase (Modified Sigma Units/mL) = 1.50 x 1.93 x 12 = 34.5.

KHM Male #3:

The absorbencies obtained were as follows:

$T_3 = 0.141$

$UB_3 = 0.013$

$RB_3 = 0.015$

Corrected $A = A_{T_3} - [A_{UB_3} + A_{RB_3}]$

$A_3 = 0.141 - (0.013 + 0.015)$

$A_3 = 0.113$

$DDF = \frac{30.3}{15} = 2.02$ Where V (mL) = 30.3.

The phenolphthalein concentration (µg/mL) was derived from the urine calibration curve and used to calculate ß-glucuronidase activity as follows:

Urine ß-glucuronidase (Modified Sigma Units/mL)

= Phenolphthalein Concentration (µg/mL) x DDF x 12.

From the urine calibration curve, the Corrected A is equivalent to a phenolphthalein concentration of 1.50 µg/mL. Thus, for KHM Male #3, the urine ß-glucuronidase (Modified Sigma Units/mL) = 1.50 x 2.02 x 12 = 36.4.

KHM Male #4:

The absorbencies obtained were as follows:

$T_4 = 0.137$

$UB_4 = 0.011$

$RB_4 = 0.013$

Corrected A = $A_{T_4} - [A_{UB_4} + A_{RB_4}]$

$A_4 = 0.137 - (0.011 + 0.013)$

$A_4 = 0.113$

$DDF = \frac{28.7}{15} = 1.91$ Where V (mL) = 28.7.

The phenolphthalein concentration (µg/mL) was derived from the urine calibration curve and used to calculate ß-glucuronidase activity as follows:

Urine ß-glucuronidase (Modified Sigma Units/mL)

= Phenolphthalein Concentration (µg/mL) x DDF x 12.

From the urine calibration curve, the Corrected A is equivalent to a phenolphthalein concentration of 1.50 µg/mL. Thus, for KHM Male #4, the urine ß-glucuronidase (Modified Sigma Units/mL) = 1.50 x 1.91 x 12 = 34.4.

KHM Male #5:

The absorbencies obtained were as follows:

$T_5 = 0.138$

$UB_5 = 0.011$

$RB_5 = 0.014$

Corrected $A = A_{T_5} - [A_{UB_5} + A_{RB_5}]$

$A_5 = 0.138 - (0.011 + 0.014)$

$A_5 = 0.113$

$DDF = \frac{30.1}{15} = 2.01$ Where V (mL) = 30.1.

The phenolphthalein concentration (µg/mL) was derived from the urine calibration curve and used to calculate ß-glucuronidase activity as follows:

Urine ß-glucuronidase (Modified Sigma Units/mL)

= Phenolphthalein Concentration (µg/mL) x DDF x 12.

From the urine calibration curve, the Corrected A is equivalent to a phenolphthalein concentration of 1.50 µg/mL. Thus, for KHM Male #5, the urine ß-glucuronidase (Modified Sigma Units/mL) = 1.50 x 2.01 x 12 = 36.2.

TABLE 2: Summary of Results Obtained From ß-Glucuronidase Urine Assay

Control Females: (results in Modified Sigma Units/mL)

#1: 15.6

#2: 14.4

#3: 15.6

#4: 15.5

#5: 15.2

Range: 14.4-15.6

Average: 15.3

Control Males: (results in Modified Sigma Units/mL)

#1: 14.4

#2: 15.4

#3: 14.4

#4: 15.4

#5: 14.4

Range: 14.4-15.4

Average: 14.8

KHM (Vohwinkel's Syndrome) Male: (results in Modified Sigma Units/mL)

#1: 35.3

#2: 34.5

#3: 36.4

#4: 34.4

#5: 36.2

Range: 34.4-36.4

Average: 35.4

The results obtained from the urine assay of ß-glucuronidase indicates that indeed a clear difference in the levels of enzymatic activity does exist when comparing healthy male and female controls to a KHM patient. According to previous studies, the normal range of β-glucuronidase urine activity is between 10-20 Modified Sigma Units/mL (Fishman et al. 1967). From our results, the levels of enzymatic activity that we obtained for both healthy adult male and female controls definitely falls within the expected normal range. It is also clear from our results that the ß-glucuronidase enzyme activity levels for our KHM male are considerably higher, almost 1.5 times higher than the control values.

The elevated level of ß-glucuronidase is a diagnostic characteristic found in patients with Vohwinkel's Syndrome. There are also several plausible explanations for why these increased levels of enzymatic activity exist. The release of ß-glucuronidase from epidermal cells may be due to a variety of different factors such as leakage, secretion, or even the actual destruction of those cells.

ß-glucuronidase is found primarily within the lysosomes of the epidermis, but may also play an important role along with other glycosidases in the lamellar bodies of the stratum corneum. The importance of glycosidases in the maturation of the stratum corneum has already been verified by studies using lectins for various carbohydrates. The findings of these studies indicate that the carbohydrate (charged sugar) residues found in the stratum granulosum are eliminated once within the stratum corneum. The removal of the charged sugar groups would create a more hydrophobic environment between the adjacent corneocytes. These intercellular spaces already have a large lipid content, but they also contain water due to the presence of these charged residues. The sugar removal also increases the non-polar lipid content since polar glycosphingolipids are converted to

non-polar lipids (Nemanic et al. 1988). While these sugar residues are present, the lamellar body network necessary for the effective occlusion of water cannot properly develop and subsequently, a breach in the water barrier layer of the epidermis occurs.

In addition, since ß-glucuronidase appears to be responsible for the normal breakdown of the hyaluronic acid component of the intercellular matrix of the epidermis (Dingle et al. 1979). This process is essential to allow the adhesion between adjacent epithelial cells to occur. ß-glucuronidase does not appear to influence the conversion of phospholipids to non-polar lipids in any way, but in excess amounts, the enzyme may appear to actually affect the glycolipids making them more polar with the addition of more glucuronic acid residues.

Another possible explanation for the elevated levels of ß-glucuronidase activity seen in KHM patients would be a possible error in the actual process of directing the enzyme to the lysosomes. It may further be postulated that the migration of ß-glucuronidase from the lysosomes into the dermal tissues could also result in the alteration of dermal ground substance thus contributing to the development of psuedo-ainhum, a characteristic symptom of many patients suffering with KHM (Camisa and Rosanna, 1984).

Thus, we see that indeed a definite relationship does exist between the elevated levels of ß-glucuronidase enzyme activity and the actual pathological process of KHM. The results from our study have clearly demonstrated a higher degree of ß-glucuronidase enzyme levels found in patients with Vohwinkel's Syndrome when compared to healthy controls. Unfortunately, there are still many unanswered questions that exist concerning Vohwinkel's Syndrome and its pathological process. Future studies in this specific area

are needed and may be able to provide definite solutions to those patients suffering from KHM.

II. *Scanning Electron Microscopy*:

The use of conventional light microscopy on routinely fixed and prepared histological sections of the skin has many severe limitations. An obvious example is the difficulty that may arise if magnification is required because of the limited resolution possible using ordinary optical systems. There is also a very limited depth of focus with light microscopy which makes proper appreciation of tissue inter-relationships extremely difficult.

In contrast, scanning electron microscopy offers a unique view of biological materials, spanning the gap between light microscopy and transmission electron microscopy. The scanning electron microscope (SEM) makes possible the exploration of large surfaces, allowing for the visualization of minute details. It yields images of tissues at magnifications up to x30,000 with great depth of field, increased resolution and a three-dimensional representation of structures. The spatial architecture and inter-relationships of various cells and tissues may be readily perceived as they occur in their living form.

In the present investigation, the scanning electron microscope has been used for the routine analysis of histologic sections of mouse ear epidermis allowing the structural characteristics of the tissue to be revealed by the exploration of the cross-sectioned surfaces.

The scanning electron micrographs clearly revealed a distinguishable epidermis surrounding a layer of elastic cartilage at low levels of magnication (Figures 1). The epidermis is characterized as a multi-layered structure with continous plaque-like layers of the stratum corneum composed of keratinized cells overlying the stratum lucidum and

stratum granulosum which are not as easily discernible. The cartilagenous layer which is "sandwiched" between the epidermal layers is composed mainly of secretory cells called chondrocytes which are usually lost during the fixation process. However, surrounding these cells are empty spaces called lacunae which are easily visible at low levels of magnification.

At higher magnification (Figure 2), the boundaries of the flattened keratinized cells of the superficial stratum corneum layer can be demonstrated.

FIGURE 1:

Cross section of mouse epidermis taken from the external ear. The elastic cartilagenous layer (C) is "sandwiched" between epidermal layers (E). The magnification is 480x and the tilt is 80°.

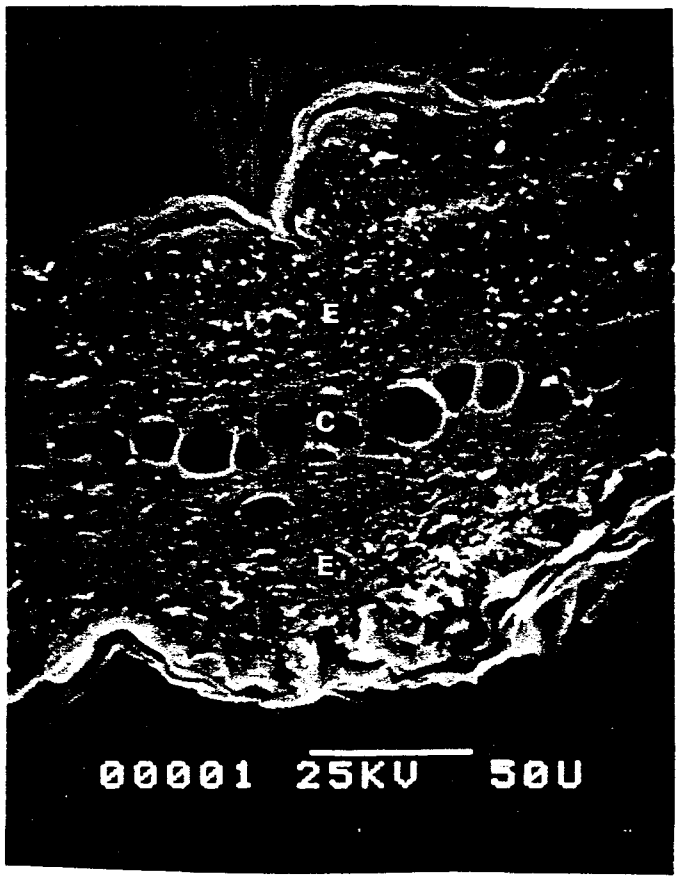

FIGURE 2:

Cross section of mouse epidermis taken from the external ear. The elastic cartilagenous layer is identified by the presence of several lacunae (L). The magnification is 1.5K and the tilt is 80°.

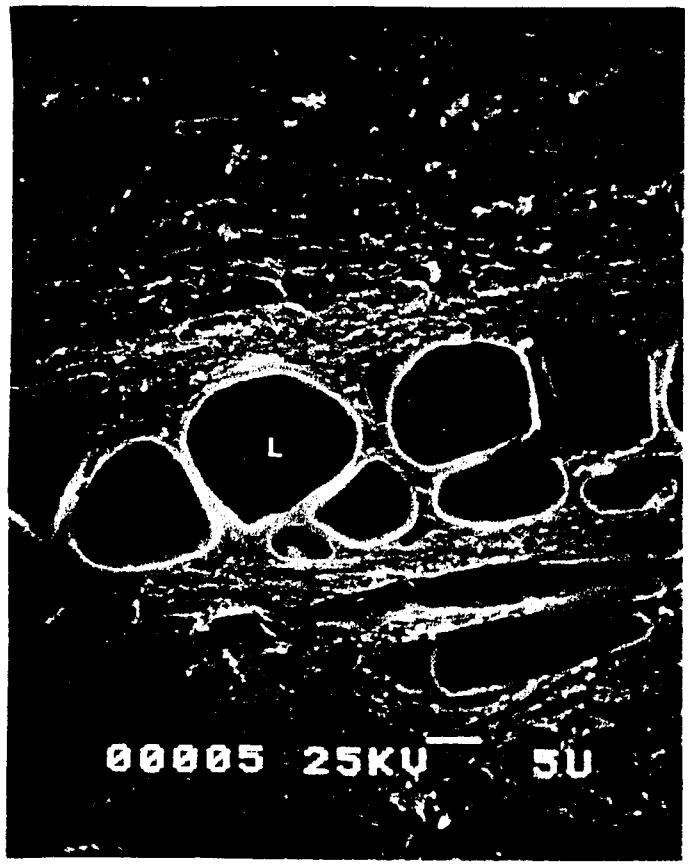

III. *Transmission Electron Microscopy:*

The main use of a transmission electron microscope (TEM) is to examine in submicroscopic detail the structure, composition and properties of biological specimens in ways that cannot be examined using other conventional equipment or techniques. The TEM is specifically utilized for examining the interior structures of biological materials at high resolution and at high levels of magnification. Thus, transmission electron microscopes can reveal the finest details of the smallest internal structures at magnifications up to x350,000.

Our current investigation employs the use of a TEM to further examine and analyze in greater depth the various components of the skin. This final phase of our microscopy research was done in two parts. The first part was an in depth study of mouse ear epidermis. The micrographs we obtained from the transmission electron microscope provided far greater detail and insight than was obtained using an SEM. The second part of our research consisted of transmission electron micrographs of normal skin which was compared and contrasted to those taken of skin with KHM.

FIGURE 3:
Cross section of mouse epidermis taken from the external ear.

A: This micrograph illustrates the ultrastructure of the epidermis. The partial thickness of the epidermis is shown at low magnification (x6000). Where the stratum corneum layer (SC), dermis (D) and keratinocyes (K) are all visible.

B: At a slightly higher magnification (x8000), greater detail is possible. The separated layers of the stratum corneum (SC) layer are quite prominently visible, as well as, the nucleus (N) of keratinocytes and the basement membrane (BM) which delineates the epidermal layers from the underlying dermis.

C: Tonofilaments (T) composed of protein cytokeratin are scattered visibly throughout the basal layer (B). The individual flattened keratinocytes of the stratum cornem layer can also be seen. The magnification is 8000x.

D: At an even higher magnification (25,000x), greater detail is possible. This micrograph allows us to see the ultrastructure of the basal layer. Where desmosomes (D), the nucleolus (N) of a basal cell and individual keratin granules (KG) within the cell can be identified.

FIGURE 3:

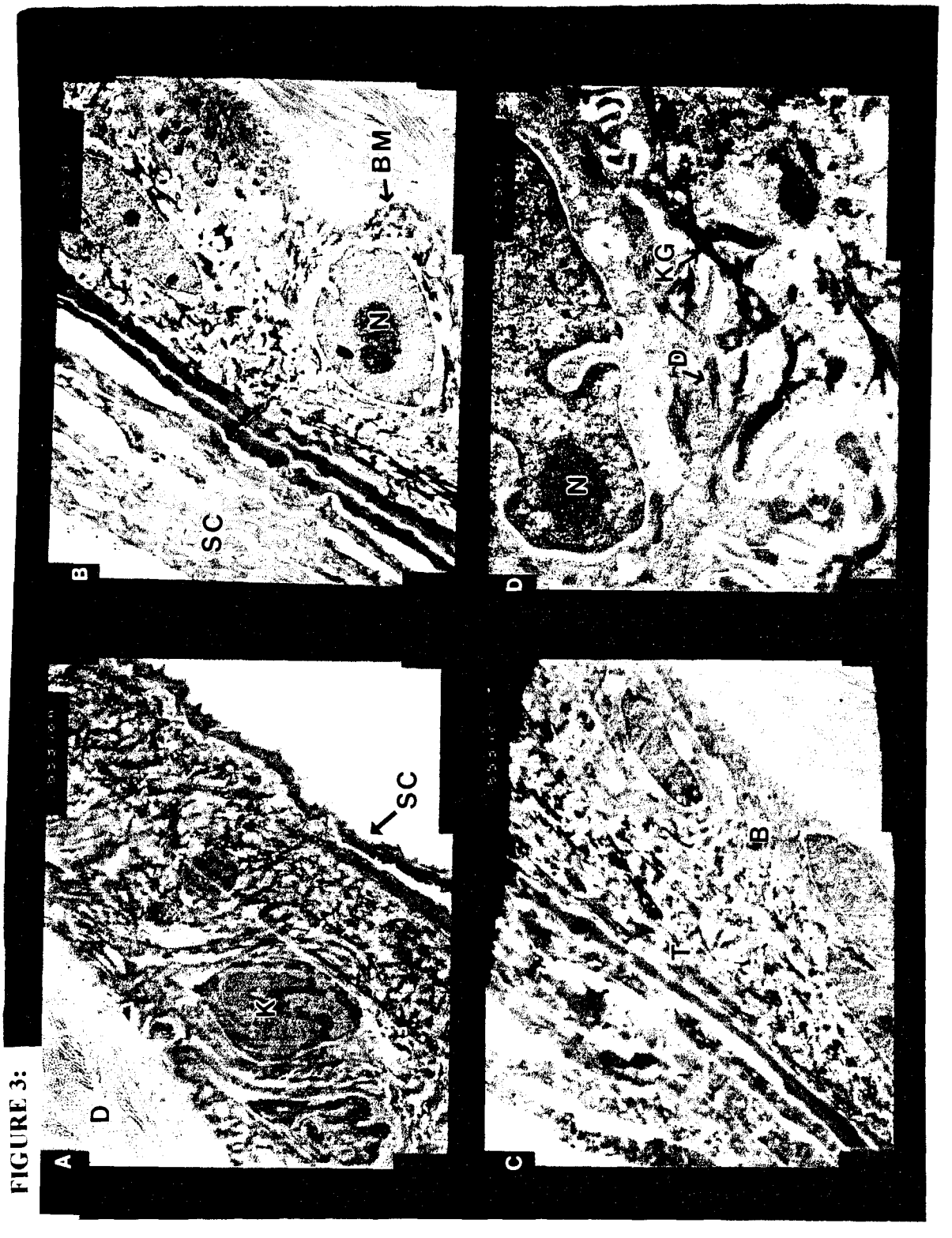

FIGURE 4:
Cross section of mouse epidermis taken from the external ear.

A: This micrograph illustrates the ultrastructure of the dermis. The dermal-epidermal junction (DJ), as well as, the basement memebrane (BM) are shown. The black "granules" interspersed throughout are mitochondria (M). The magnification is 30,000x.

B: At a magnification of 25,000x, desmosomes (D) are clearly depicted. The visible cell is a fibroblast (F) found in the dermal layers.

C: Collagen fibers (CF) found in the dermis are quite prominent in this micrograph. A partial fibroblast (F) can be seen in the lower right corner. The magnification is 30,000x.

D: At an even higher magnification (35,000x), greater detail is possible. This micrograph allows us to see the ultrastructure of the underlying dermal layers. The dark irregular shaped structure is a melanocyte (M). Its intercellular cytoplasm (IC) is depicted as an amorphous darkly colored mass within the cell.

FIGURE 4:

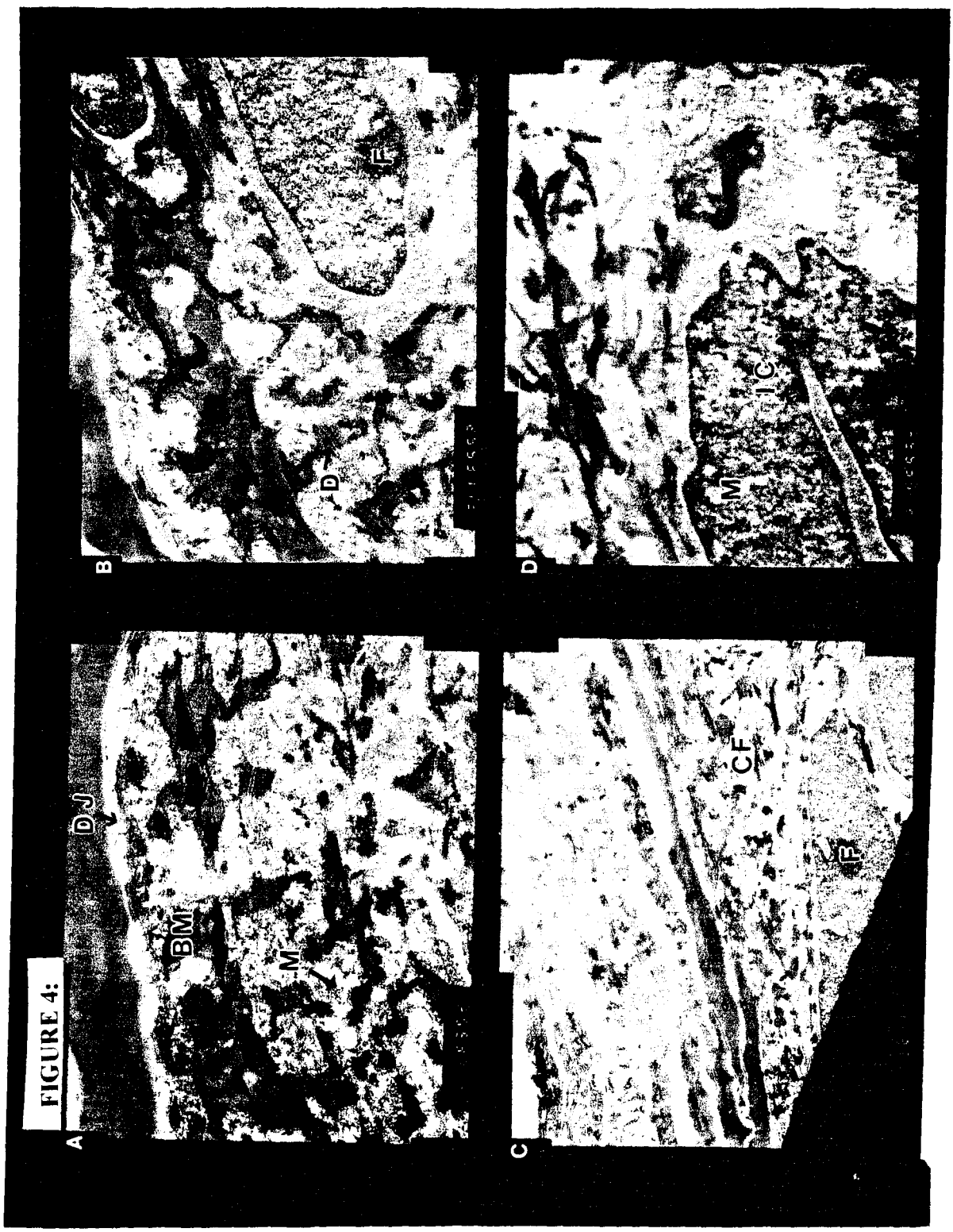

FIGURE 5:
Cross section of mouse epidermis taken from the external ear. This montage illustrates one complete cell, a keratinocyte (K). The keratohyalin granules (KG) are the very irregularly shaped, dark amorphous masses found along the periphery of the nucleus (N) and extending from either end of it. The cell in the montage appears to be up against the cornified layers of the skin (the dark gray band running along the top). A faint line denoting a basement membrane (BM) can be seen, as well as, several desmosomes (D) interspersed throughout. The magnification is 30,000x.

FIGURE 5:

FIGURE 6:
This series of micrographs was taken from normal dry human epidermis.

A/B: These micrographs illustrate the ultrastructure of the stratum granulosum or the granular layer (G). The cells found in this layer appear slightly flattened. This layer is characterized by dense protein granules called keratohyalin (K) and also contains large quantities of tonofibrillar materials (T). The partial thickness of the epidermis is shown at low magnification (x3000).

C: At an even higher magnification (8000x), visualization is much easier. The nucleus (N) of the granular cell is quite distinct. Where keratohyalin granules (K) and tonofibrils (T) can also be seen.

D: This micrograph illustrates the region near the dermal-epidermal junction (DJ). Several basal cells (B) with their nuclei (N) are visible. The dermal layers are characterized by the presence of collagen fibers (C) produced by fibroblasts (F). The magnification is 3000x.

FIGURE 6:

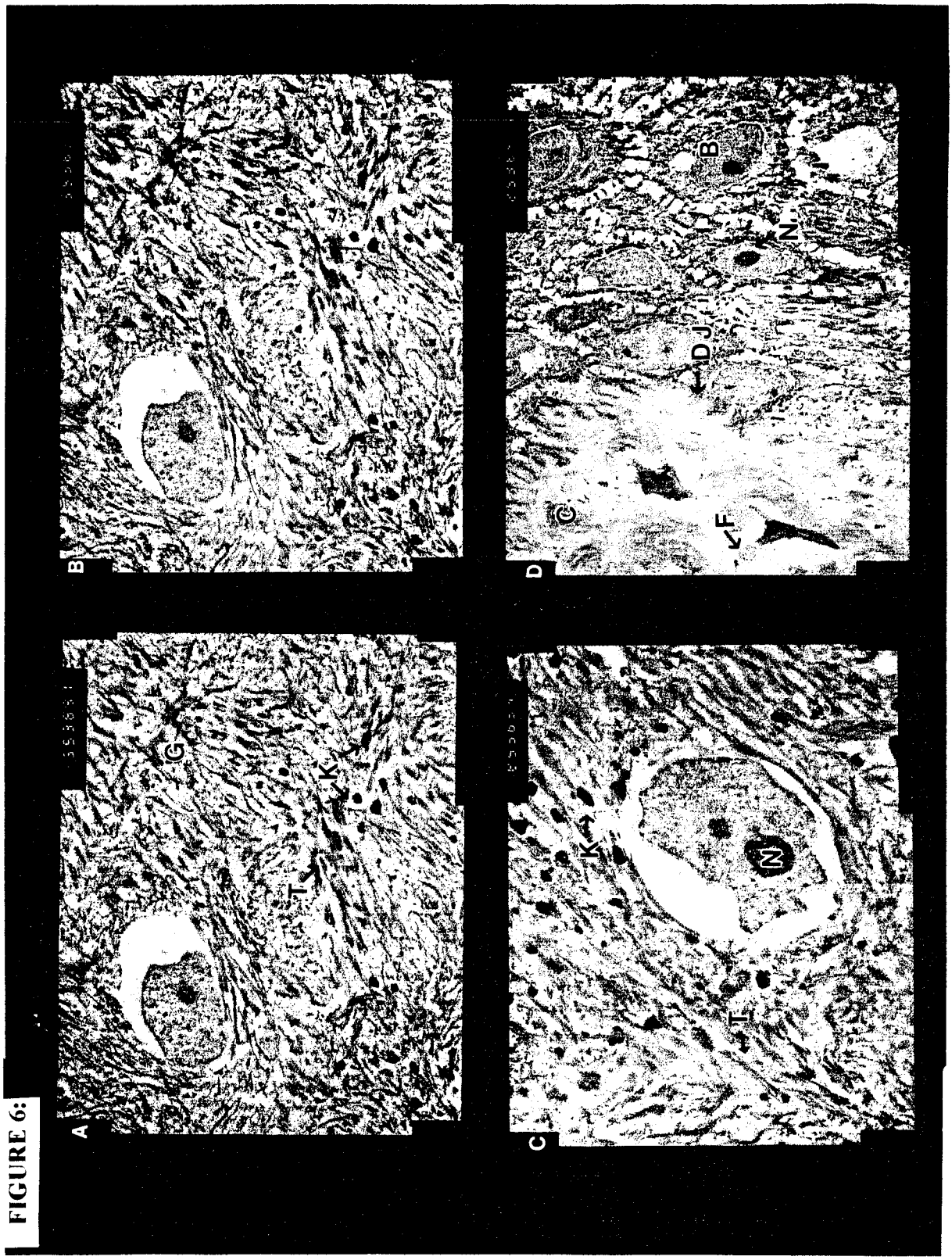

FIGURE 7:
This series of micrographs was taken from normal dry human epidermis at a magnification of 2000x. This montage illustrates the cytological details of the various layers comprising the epidermis. The stratum corneum layer (SC), seen on the far left of the montage, is characterized by morphology that is strikingly different from that of the underlying layers. The dead and dying cells are flattened, devoid of nuclei and other organelles and filled with mature keratin. In contrast, the cells of the stratum granulosum (SG) are characterized by numerous dense granules known as keratohyalin granules. The stratum spinosum (SS), also known as, the "prickle cell" layer contains cells that are relatively large and polyhedral in shape with prominent nuclei. Tonofibrils (T) also appear in this layer. The layer most adjacent to the dermis is the stratum basale (SB) which contains cells that are cuboidal in nature and form a single layer separated from the dermis by a basement membrane (BM). Underlying these epidermal layers, the dermis is characterized by its high content of collagen fibers (CF) and fibroblasts.

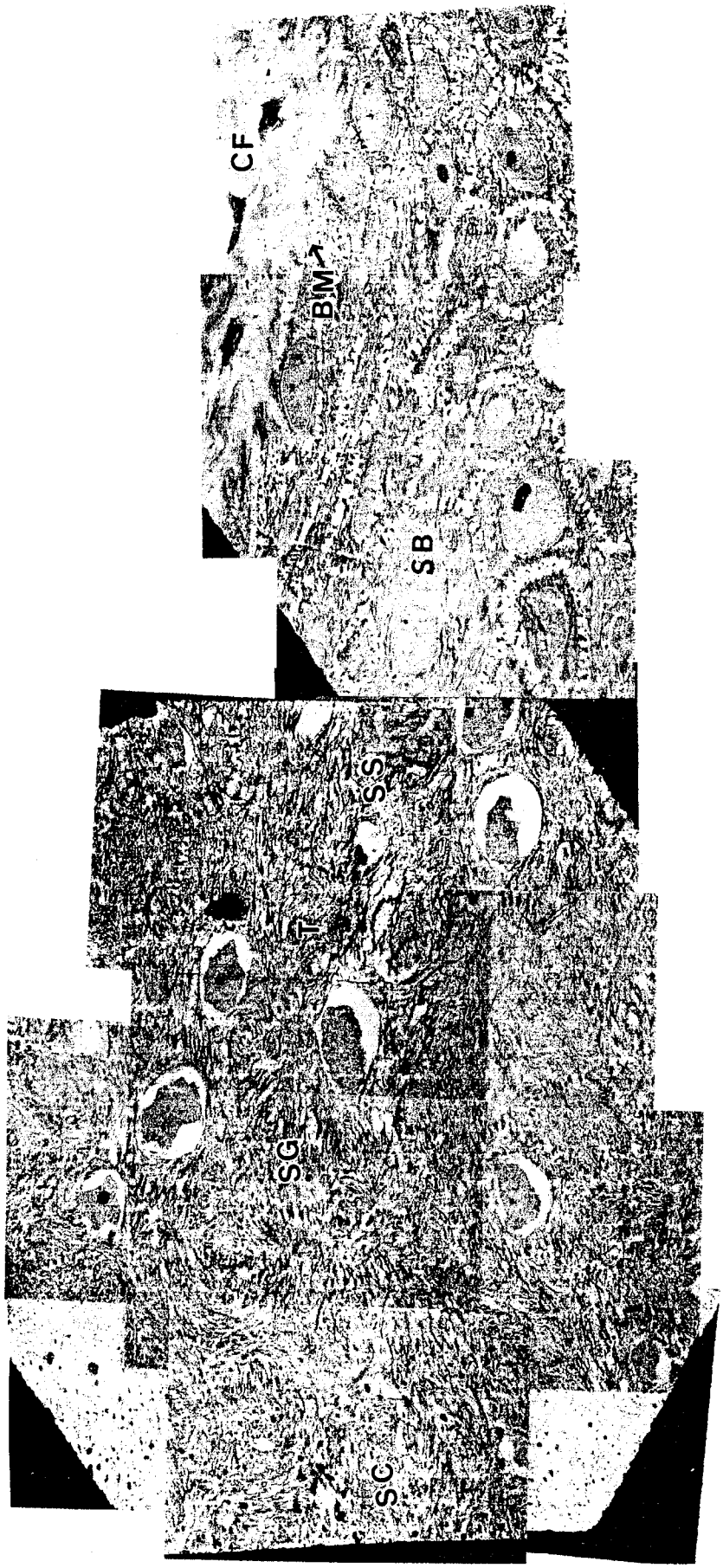

FIGURE 7:

FIGURE 8:
These micrographs represent dry human epidermis taken from an adult male with Vohwinkel's Syndrome (KHM). In comparison to micrographs taken of dry normal human skin, the changes in KHM skin are quite notable. The stratum corneum (SC) layer is marked by hyperkeratosis (H) of the keratin with patchy regions of hypergranulosis. The presence of large irregular keratohyalin granules (K) which appear clumped in appearance characterizes a very prominent stratum granulosum (SG) layer. The presence of cells with a highly vacuolated appearance is characteristic of KHM patients as well. The cellular nuclei appear extremely pyknotic and are usually absent in heavily damaged regions. The overall cellular mitotic activity is much greater than normal epidermis. The stratum spinosum (SS) and the stratum basale (SB) layers are marked by an increase in the number of tonofilaments (T). The dermal layers remain unaffected.

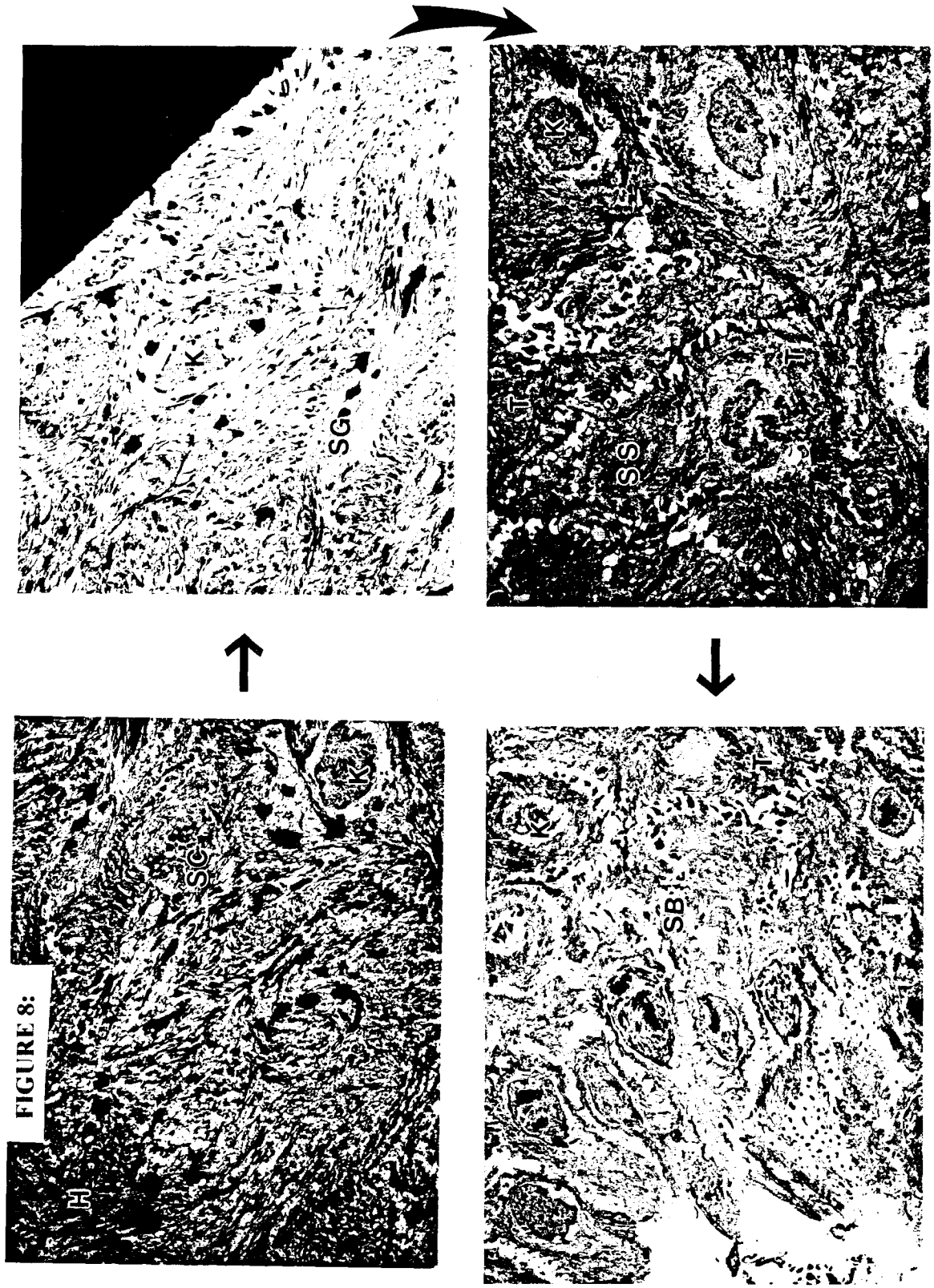

FIGURE 8:

FIGURE 9:
These micrographs represent dry human epidermis taken from an adult male with Vohwinkel's Syndrome (KHM).

A: At a magnification of 50,000x, the presence of a large irregularly shaped keratohyalin granule is indicative of KHM patients. The granule also has its characteristic clumped appearance.

B: In the stratum granulosum, the presence of a granular cell (C) is noted. Unlike normal epidermal cells, the nucleus is absent. Large vacuolated cells (V) make their appearance as well. The increased number of tonofilaments (T) in this region are also visible, as well as, numerous keratohyalin granules (K). The magnification is 8000x.

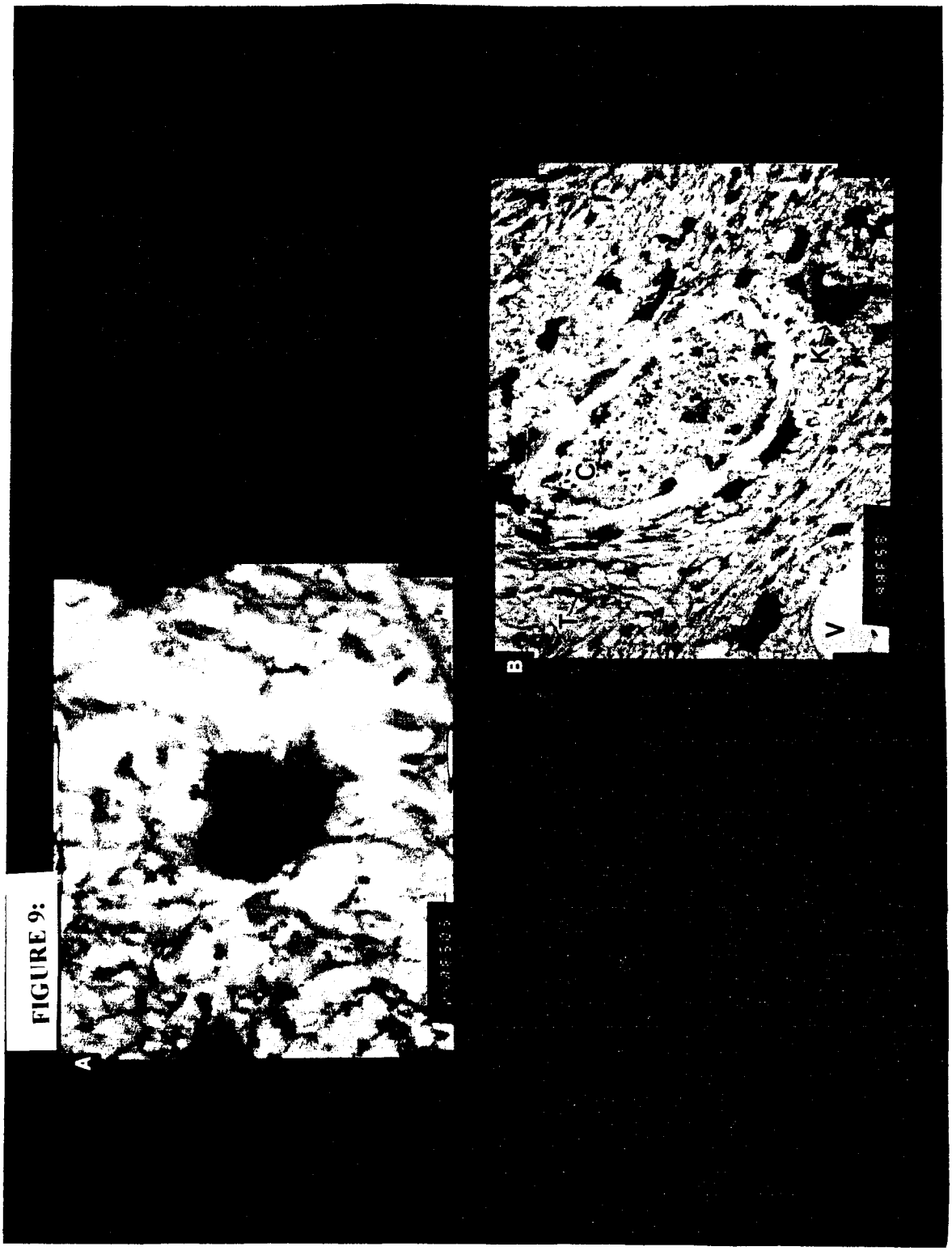

FIGURE 9:

FIGURE 10:
These micrographs represent normal human epidermis taken from an adult male hand that has been soaked in water for 20 minutes. Very little difference is noted when compared to completely dry epidermis of normal skin due to the effects of the water barrier. The epidermal layers present are the stratum lucidum (SL), stratum granulosum (SG), stratum spinosum (SS) and the stratum basale (SB) layer. The immersion in water, regardless of the time spent has almost no effect on the epidermal layers of normal skin. The magnification is 2000x.

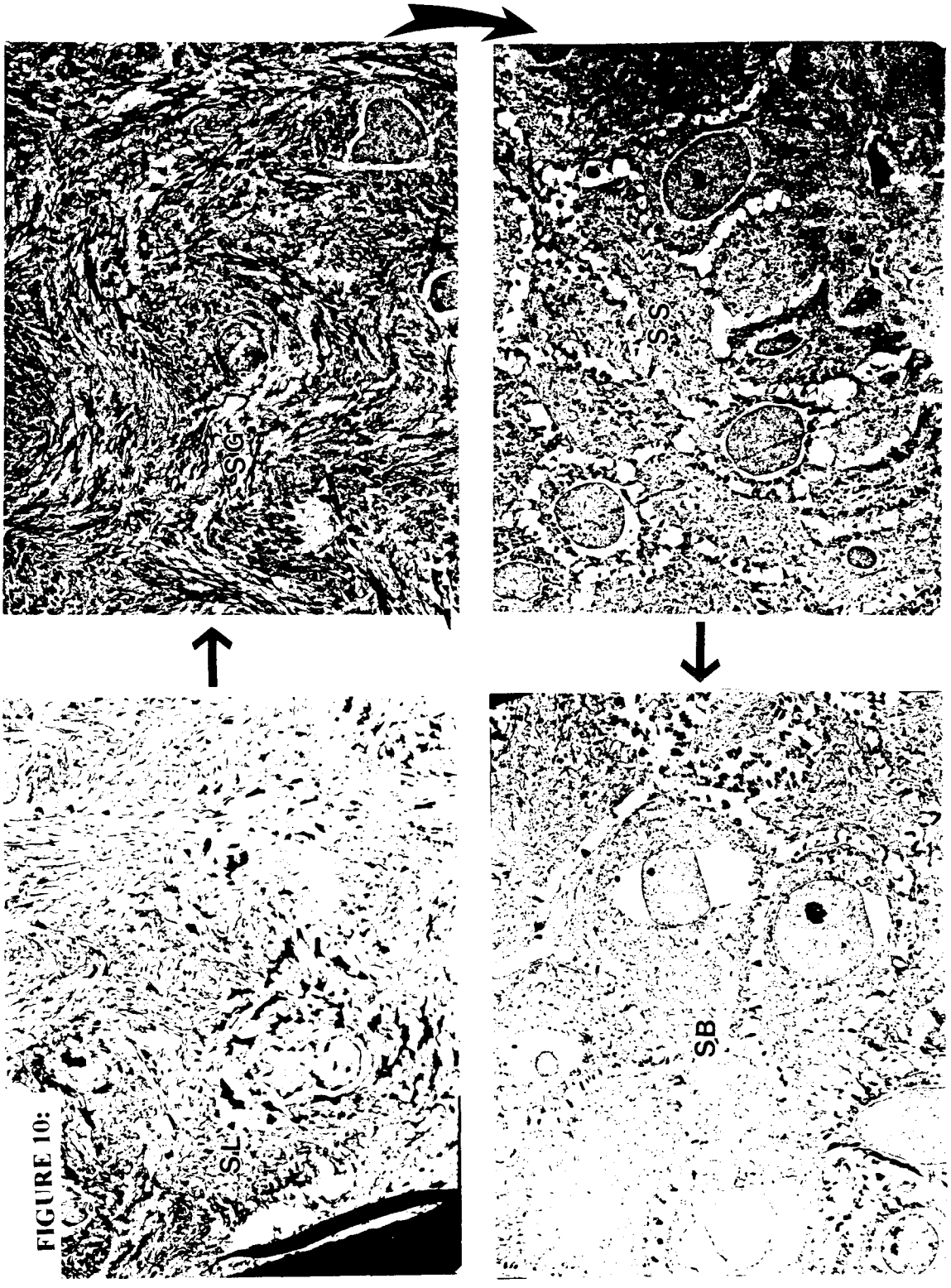

FIGURE 10:

FIGURE 11:
These micrographs represent human epidermis taken from an adult male hand with KHM that has been soaked in water for 20 minutes. The magnification is 2000x. A marked difference when compared to normal skin is noted. The stratum corneum (SC) layer is marked by hyperkeratosis (H) of the keratin with patchy regions of hypergranulosis. The presence of large irregular keratohyalin granules (K) which appear clumped in appearance characterizes a very prominent stratum granulosum (SG) layer. The presence of cells with a highly vacuolated appearance is characteristic of KHM patients as well. The cellular nuclei appear extremely pyknotic and are usually absent in heavily damaged regions. The overall cellular mitotic activity is much greater than normal epidermis. The stratum spinosum (SS) and the stratum basale (SB) layers are marked by an increase in the number of tonofilaments (T). The dermal layers remain unaffected.

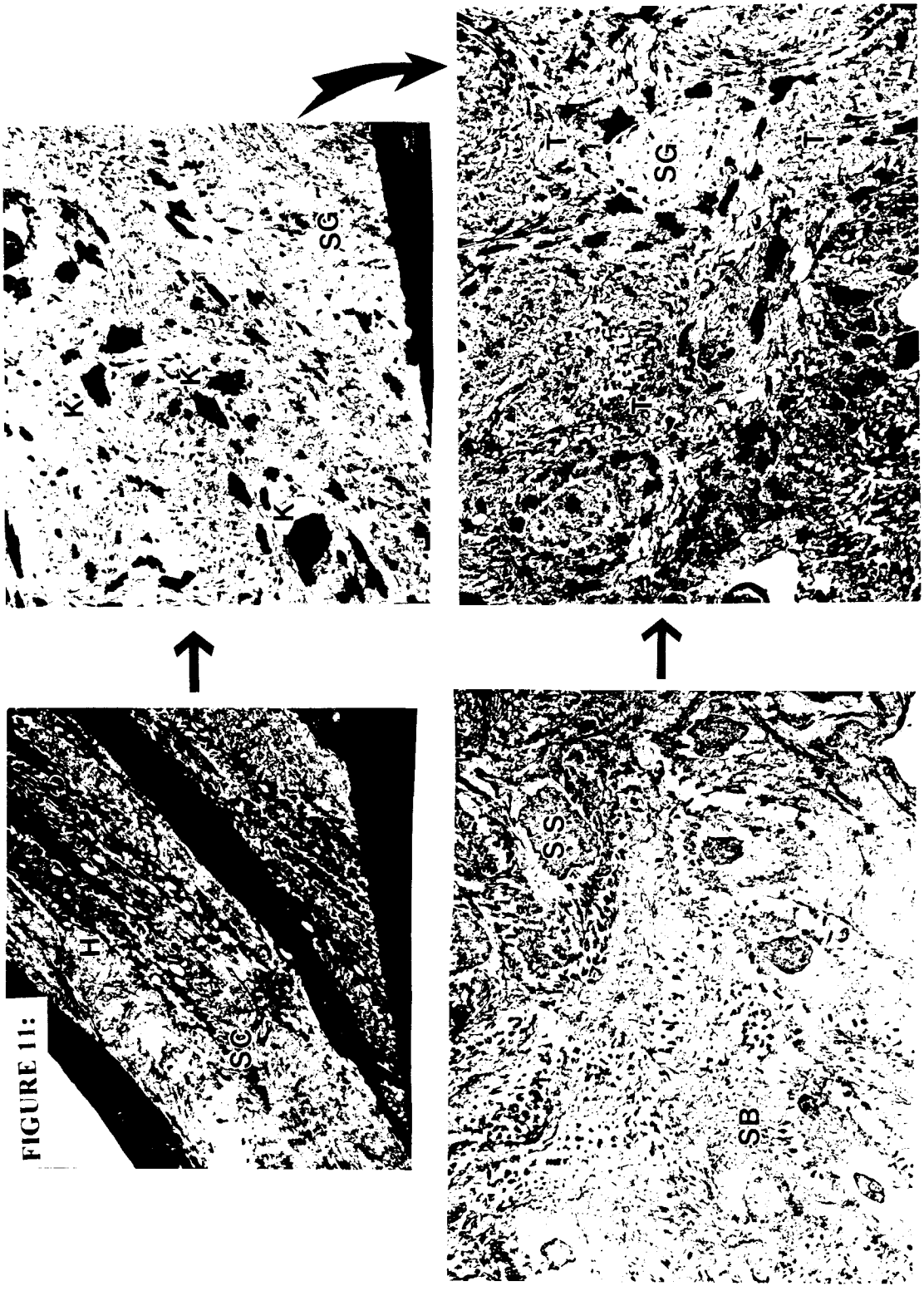

FIGURE 11:

FIGURE 12:
These micrographs represent human epidermis taken from an adult male hand with KHM that has been soaked in water for 20 minutes. The specific layers of the epidermis pictured are the stratum corneum (SC) and the stratum granulosum (SG). The stratum corneum is characterized by marked areas of hyperkeratosis (H) which appear black in the micrographs. The stratum granulosum is marked by a number of very irregularly shaped vacuolated cells lacking a nucleus. The number and density of tonofilaments (T) has also increased. The magnification is 2000x.

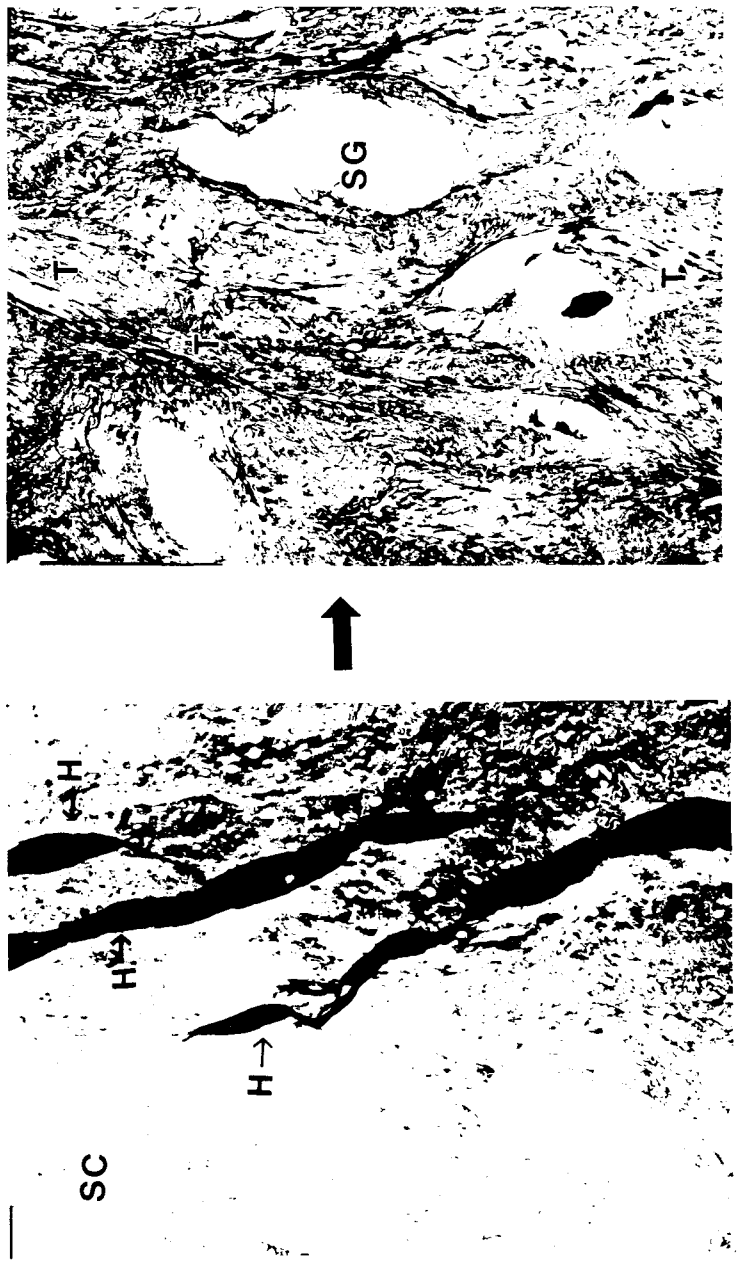

FIGURE 12:

FIGURE 13:
This montage represents human epidermis taken from an adult male hand with KHM that has been soaked in water for 20 minutes. The specific layers of the epidermis pictured are the stratum corneum (SC), the stratum lucidum (SL) and the stratum granulosum (SG). The stratum lucidum is an extremely thin homogeneous layer found between the stratum corneum and the stratum granulosum in thick skin only. It is usually very difficult to see in normal skin. However, this micrograph of KHM skin illustrates a very well developed and prominent stratum lucidum. Also visible are areas containing a high number of keratohyalin granules (K). The magnification is 5000x.

FIGURE 13:

FIGURE 14:
These micrographs represent human epidermis taken from an adult male hand with KHM that has been soaked in water for 20 minutes. The specific layers of the epidermis pictured are the stratum granulosum (SG), the stratum spinosum (SS), the stratum basale (SB) and the dermis (D). The stratum granulosum is marked by a very high number of irregularly shaped vacuolated cells lacking a nucleus. The number and density of tonofilaments (T) and keratohyalin granules (K) has also increased. Both the stratum spinosum and stratum basale show an increase in cellular activity illustrated by the dark regions. The lack of distinct cells with nuclei is apparent. These regions lack the normal organization and ultrastructure found in normal human epidermis. The magnification is 3000x.

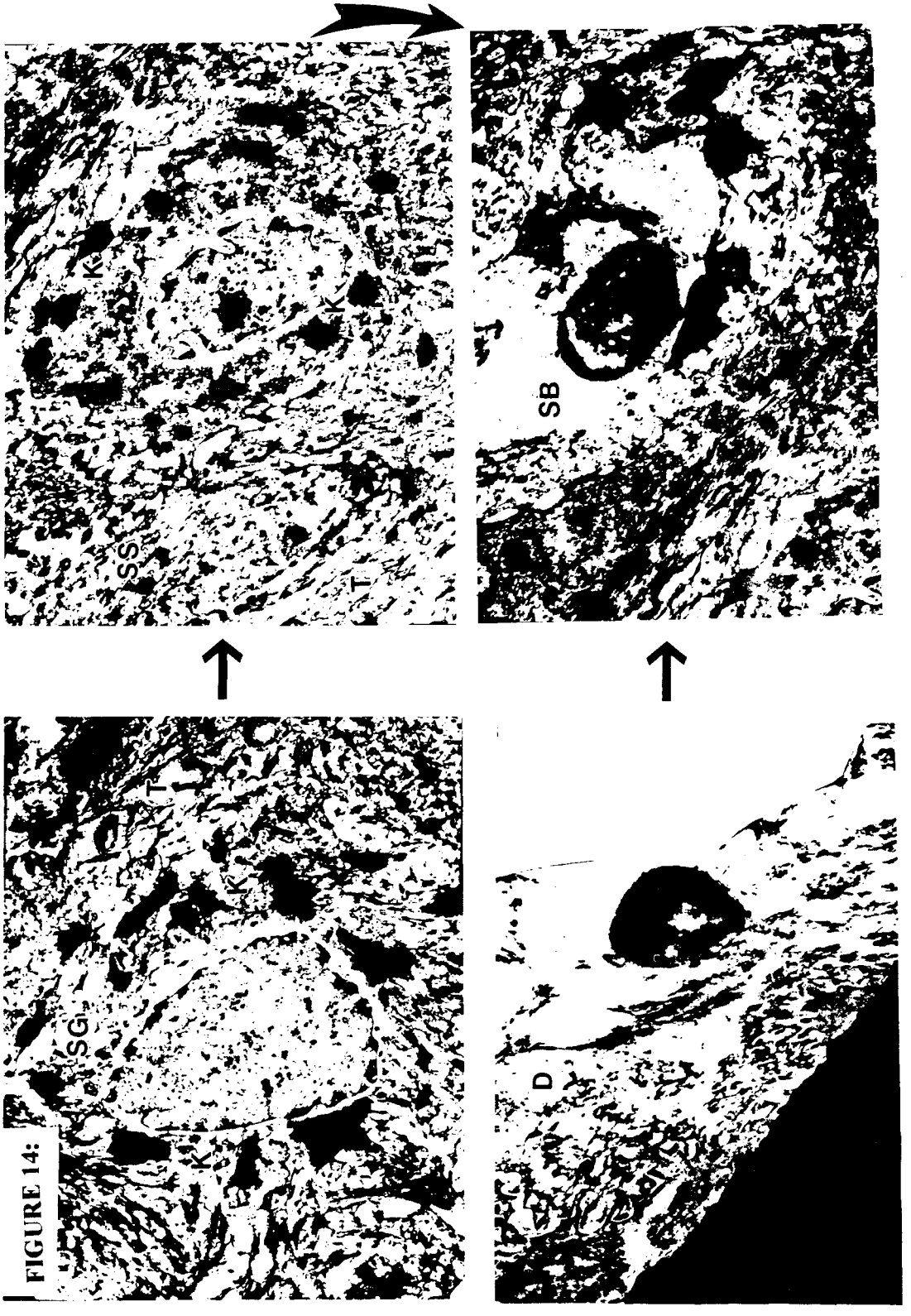

FIGURE 14:

IV. *Immunoelectron Microscopy*:

Immunoelectron microscopy revealed that staining with an antibody specific for the N-terminal domain of the loricrin protein indicated that the positive cell layer in the skin biopsy from an affected patient was markedly thickened compared to normal skin. Within the granular cells of normal skin, loricrin is diffusely distributed and specific loricrin immunoreactive granules were frequently observed within the nuclei of the granular cells. The cornified envelopes of normal skin were intensively labeled with loricrin antibody, while those from the Vohwinkel's Syndrome (VS) patients were less frequently labeled.

These findings indicate that in the patient's skin, loricrin is abnormally or less efficiently incorporated in to the cornified envelope (CE) and is found to accumulate in intranuclear granules. Therefore, even though the deposition of loricrin into the CE is abnormal, the overall formation of a proper CE scaffold is not prevented in these patients. These findings are consistent with the hypothesis that loricrin is involved in the late steps of CE assembly, and the mutation is more than likely to affect the stabilization of the CE mediated by the attachment of loricrin to the inner surface of the CE scaffold (Maestrini et al. 1996). It has also been hypothesized that loricrin mediates the interaction of the CE with keratin intermediate filaments providing the anchorage and coordination of the two structures. This interaction may be mediated by the association of glycine-loop motifs which are present in loricrin. In addition, keratin or filaggrin molecules are also specifically cross-linked to loricrin in the CE (Steinert and Marekov, 1995). This interaction could be impaired by the defect in loricrin, causing destabilization and disruption of the entire cellular structure. More specifically, it is possible that the

inability to cross-link keratin intermediate filaments with loricrin in the CE interferes with normal function of the cornified layer and leads to hyperkeratosis. It is also interesting to note that loricrin is expressed in epidermal cells throughout the body (Hohl et al. 1993).

The silver enhanced-colloidal gold-loricrin reactive particles were observed as large, specific electron-dense particles measuring approximately 10-100 nm in diameter and were easily observed by EM technique even at low levels of magnification. The most striking abnormality was the presence of the intranuclear granules visible in the upper granular cell layers (Figure 15A). Although these granular cell layers were thickened, the keratohyalin granules appeared quite normal (Figure 15A). The transitional cell layer, which is only occasionally observed in normal healthy skin, was quite distinct and can be seen quite clearly in between the granular and cornified cell layers. The presence of lamellar granules was also increased in number within the spinous and granular cell layers. In addition, thin electron-dense cell envelopes were seen in the superficial granular cell layer. However, the increase in thickness of the cellular envelopes within the CE layer of normal skin was not observed in the skin of VS patients (Figure 15B).

To identify the composition of the granules, immunoelectron microscopy was performed to show that the intranuclear granules in the granular cell layers were loricrin immunoreactive (Figure 16A). The retained nuclei in the parakeratotic cornified cellular layer also contained loricrin positive granules (Figures 17A and 17C). However, the cornified cell envelopes were very sparsely labeled with the loricrin antibody (Figures 17B and 17C), which was in complete contrast to the labeling pattern seen within normal

skin where the loricrin antibodies intensely seem to decorate the cornified cell envelopes (Figure 17D). The most superficial granular cells or transitional cells of the patient's skin often showed more loricrin labeling on the cellular envelopes than in the matured cornified cells (Figure 17B). This pattern has not been observed in the normal skin and is in keeping with the aberrant cornified cell envelope assembly.

FIGURE 15:

Electron microscopy showing abnormal epidermal differentiation in the patient's skin.

A: Superficial granular cell layer containing many characteristic intranuclear granules (arrowheads). Where T: transitional cell layer, * denotes the presence of increased intercellular substance derived from lamellar granules, K: keratohyalin granules, L: lipid droplets, and N: nucleolus. The Bar = 0.1 μm.

B: The cornified cell envelopes (arrows) in the patient's skin, are thinner than in normal skin (Inset showing a healthy case). Where D: desmosomes. The Bar = 0.1μm.

FIGURE 15:

FIGURE 16

Immunoelectron microscopy showing abnormal loricrin staining in VS patient skin: loricrin labeling in granular cells. Immunoreaction is heavily accumulated on the intranuclear aggregates (arrowheads) in patient skin. Normal skin shows diffuse cytoplasmic and nucleoplasmic labels not associated with the granules.

A: VS patient

B: Healthy individual

Where N: nuclei. The Bar = 1.0 μm.

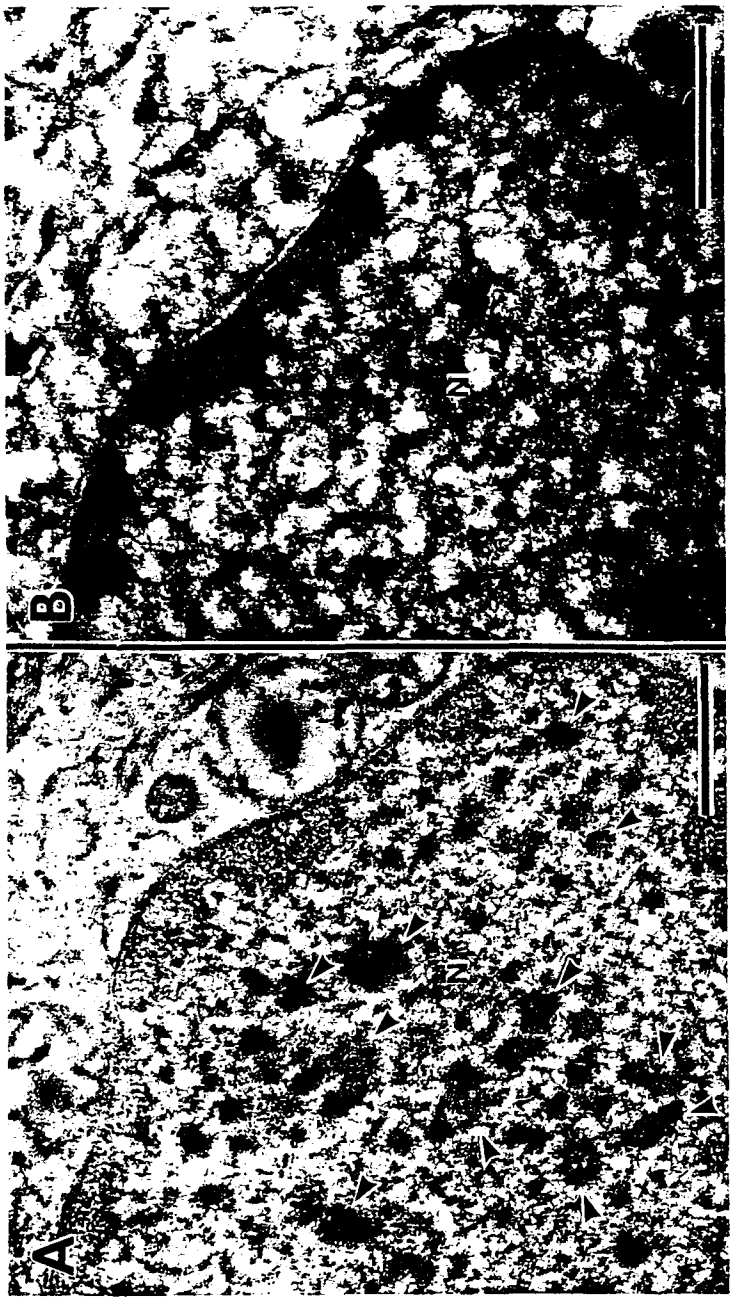

FIGURE 16:

FIGURE 17:

Loricrin (labeled with 5 nm colloidal gold) staining demonstrated aberrant cornified cell envelope formation. The areas marked by boxed numerals "1" and "2" in A are shown at a higher magnification than B and C. Note both the temporal cell peripheral accumulation of loricrin labels (Arrows in B) in the most superficial granular cells and disappearance of the labels on the cell envelope of the cornified cells in the VS patient's skin. Compare that with rich loricrin labeling in normal cornified cell envelopes (Figure D). Where * denotes granular aggregates within parakeratotic cornified cell nucleus are densely labeled with the loricrin antibody (Figure C).

C: (Arrows) May depict other cellular proteins (involucrin) on the cornified cell envelope which are abundant in the VS patient's skin (Figures B and C) but not in normal skin (Figure D). Where G: granular cells, C: cornified cells, N: nuclei, A-C depicts patient biopsy skin and D is healthy skin. The Bar is 5 μm in A and 0.1 μm in B, C and D.

FIGURE 17:

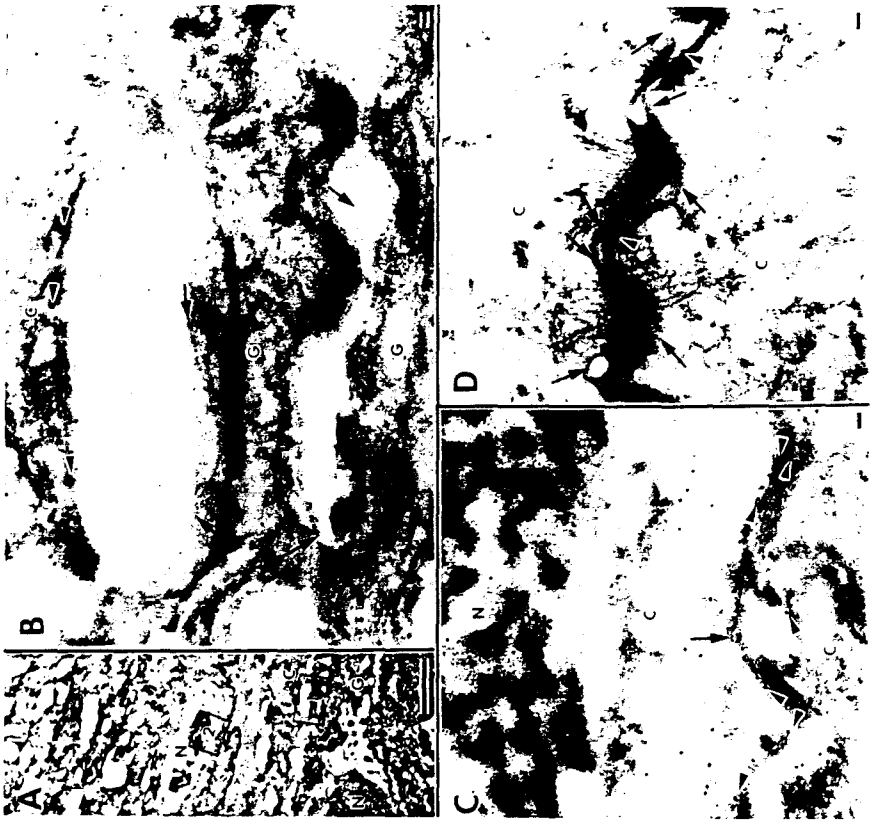

Discussion

Keratoderma Hereditaria Mutilans (KHM) or Vohwinkel's Syndrome is an autosomal dominant genodermatosis characterized primarily by a defect in the process of keratinization. K. Vohwinkel was the first to describe this rare and unique pathological process in 1929. This research is an attempt to focus on the exact nature of Vohwinkel's Syndrome with an emphasis on the histological aspects of the epidermal layers through the use of an electron microscope. The current investigation clearly demonstrates histologically the differences found when comparing KHM epidermis to normal epidermis.

Previous work done by Camisa and Rosanna (1984) clearly revealed the differences that exist between healthy skin and KHM skin. They also successfully demonstrated the variations found throughout the different epidermal layers within KHM skin. Ultrastructurally, our EM findings illustrated that the entire epidermis is affected in patients with KHM. Many significant changes and variations can be seen throughout the stratum corneum, the stratum granulosum, the stratum spinosum and the stratum basale layers. Only the underlying dermis seems to remain unaffected.

The preceding micrographs allowed us to examine and analyze the various changes in structure, organization, composition and thus, the overall nature of KHM skin. A characteristic histological picture is visualized within the epidermis. Previous research done by P.M. Elias extensively examined the exact nature of the stratum corneum layer. Elias further identified the presence of specific lipids and their importance in the maintenance of the water barrier. Further studies by Onken and Moyer (1963), Joseph C.

Mackenzie (1969), Scheuplein and Blank (1971), as well as, Serri and Montagna (1972) clearly demonstrated the importance of the permeability barrier as an integral part of normal functioning epidermis. Wilgram and Caufield (1987) employed the electron microscope as an effective tool in the study of various epidermal diseases.

The stratum corneum is characterized by extreme hyperkeratosis. Naturally, the overall thickness and density of this specific layer has been greatly expanded due to the increase in keratinization. Underlying this zone of hyperkeratinization, the effects become even more obvious. Most evident are the variously sized clear spaces surrounding the nuclei in the upper stratum spinosum and in the stratum granulosum, the two regions that seem to be the most affected. Our EM findings showed that these clear spaces or vacuolated areas (which are electron-light in nature) were most likely areas of cytoplasm that lacked the characteristic tonofilaments but were instead filled with an abundance of cellular organelles including ribosomes, glycogen particles, mitochondria, multivesicular bodies and keratinosomes distributed within a loose fibrillar matrix rather than being distributed in their normal diffuse pattern throughout the cytoplasm. In contrast, areas that appeared electron-dense in the micrographs consisted primarily of abnormal clumps of tonofilaments and keratohyalin protein. The micrographs also illustrate that peripherally located to these clear spaces, indistinct cellular boundaries were formed by the clumping of dense irregularly shaped keratohyalin granules. The keratohyalin protein seemed to be prematurely deposited on the tonofilament masses to produce large keratohyalin-tonofilament complexes. These complexes persisted into the lower layers of the epidermis. The markedly thickened stratum granulosum layer clearly illustrates an increased number and density of these oversized keratohyalin-tonofilament

complexes. The desmosomes appeared to be intact, and there appeared to be no separation of epidermal cells from one another. There also appeared to be a lack of cytolytic vacuoles in the lower epidermis and the upper dermis appeared completely normal. In addition, basal keratinocytes and spinous cells appeared normal in structure, although there was a marked redundancy of the basal lamina at the dermo-epithelial junction. The variations introduced above are definitely lacking in normal human epidermis. It is now clear that the stratum corneum undergoes a series of alterations during its journey from the lower layers of the epidermis to the superficial layers, with each modification contributing to the overall outcome in regards to structure, function and composition of the epidermis as a whole.

In recent years, enormous progress has been made in the investigation of skin diseases. The discovery and demonstration of a specific loricrin mutation in the pathological process of Vohwinkel's Syndrome provides clear evidence that the proper formation of the cornified envelope is essential for normal skin function. Dr. A. Ishida-Yamamoto et al. (1998) focused their research primarily on the underlying cause of KHM, which can now be attributed to a frameshift mutation within the loricrin gene. In addition, research done by Akiyama et al. (1998) further demonstrated the importance of the cornified envelope, its function and its relationship to the water barrier.

Further identification of the exact genetic basis of VS will allow scientists and physicians to prescribe better treatment for these patients in the future. Currently, the majority of patients with VS respond well to systemic retinoid therapies. More specifically, the retinoic acid suppresses the expression of the defective loricrin protein (Hohl, Mehrel et al. 1991). Further research and study in this area will hopefully allow

for the development of specific drugs which specifically suppress loricrin expression with less side effects than retinoic acid, since retinoids also inhibit the expression of other cornified envelope precursor proteins. The detection of the precise nature of the mutation is a great step forward in the development of a possible future gene therapy against Vohwinkel's Syndrome.

Our investigation barely scratches the surface of this mysterious and quite elusive pathological process. It is our hope that the future will hold some positive answers for the many people currently suffering from KHM.

WORKS CITED

Akiyama, Matashi., Angela M. Christiano, Kozo Yoneda and Hiroshi Shimizu. 1998. Abnormal Cornified Cell Envelope Formation in Mutilating Palmoplantar Keratoderma Unrelated to Epidermal Differentiation Complex. *J Invest Derm*. 111(1): 133-138.

Albert, Frank I., Chang Sing Pang, Arnold P. Oranje, Vojislav D. Vuzevki and Ernst Stolz. 1981. Successful Treatment of KHM with an Aromatic Retinoid. *Arch Derm*. 117: 225-228.

Altman, Lawrence G., Barbara G. Schneider and David S. Papermaster. 1984. Rapid Embedding of Tissues in Lowicryl K4M for Immunoelectron Microscopy. *J Histochem Cytochem*. 32(11): 1217-1223.

Bancroft, Joseph D. Histochemical Techniques; 2nd Ed. Boston: Butterworths Publishers, 1975. pgs. 292-302.

Bassett, F. 1976. Function and Characteristics of Langerhans Cells. *Arch Derm*. 102: 280-292.

Baumberger, Joseph Peter, V. Suntzeff and E.V. Cowdry. 1978. Separation of Epidermis from Dermis. *J Nat Cancer Inst*. 51: 413-423.

Bendayan, Moise and Max Zollinger. 1983. Ultrastructural Localization of Antigenic Sites on Osmium-fixed Tissues Applying the Protein A-Gold Technique. *J Histochem Cytochem*. 31(1): 101-109.

Bergfeld, Wilma F., V.J. Derbes, P.M. Elias, P. Frost, K.E. Greer and J.L. Shupack. 1982. The Treatment of Keratosis Palmaris et Plantaris with Isotretinoin. *J Am Acad Derm*. 6: 727-731.

Bickenbach, Jackie R., Jeanette M. Greer, Donnie S. Bundman, Joseh A. Rothnagel and Dennis R. Roop. 1995. Loricrin Expression Is Coordinated with Other Epidermal Proteins and the Appearance of Lipid Lamellar Granules in Development. *J Invest Derm*. 104(3): 405-409.

Blanchet-Bardon, C., Vincenzo Nazzaro, Charles Rognin, Jean-Marie Geiger and Antoine Puissant. 1991. Acitretin in the Treatment of Severe Disorders of Keratinaization. *J Am Acad Derm*. 24: 982-986.

Blasik, L.G., R.L. Dimond and R.D Baughman. 1981. Hereditary Epidermolytic Palmoplantar Keratoderma. *Arch Derm*. 117: 229-231.

Bohnert, Axel and Ingrun Anton-Lamprecht. 1982. Richner-Hanhart' Syndrome: Ultrastructural Abnormalities of Epidermal Keratinization Indicating a Causal Relationship to High Intracellular Tyrosine Levels. *J Invest Derm*. 79(2): 68-74.

Camisa, Charles and Cindy Rosanna. 1984. Variant of KHM (Vohwinkel's Syndrome). *Arch Derm*. 120: 1323-1328.

Camisa, Charles and H. Williams. 1985. Epidermolytic Variant of Hereditary Palmoplantar Keratoderma. *Br J Derm*. 112: 221-225.

Candi, Eleonora., Gerry Melino, Giampiero Mei, Edith Tarcsa, Soo-Il Chung, Lyuben N. Marekov and Peter M. Steinert. 1995. Biochemical, Structural, and Transglutaminase Substrate Properties of Human Loricrin: The Major Epidermal Cornified Cell Envelope Protein. *J Biol Chem*. 270(44): 26382-26390.

Cole, Richard D., Michael G. McCauley and Barbara H. Way. 1984. Vohwinkel's KHM. *Int J Derm*. March(2): 131-134.

Cunliffe, William J. and Andrew J. Miller. Retinoid Therapy. England: MTP Press Limited. 1984.

Dicken, Charles H. 1984. Retinoids: A Review. *J Am Acad Derm*. 11(4): 541-552.

Dingle, Jeremy T., Paul J. Jacques and I. H. Snow. 1979. Lysosomes in Applied Biology and Therapeutics. *Histochem J*. 119: 65-77.

Duke, Edgar E., Douglas W. Justus and J. K. Rivers. 1985. Etretinate: The Management of KHM in Four Family Members. *J Am Acad Derm*. 13: 43-49.

Ebner, Phillip. 1977. Distribution of Langerhans Cells. *J Anat*. 198: 159-172.

Elias, P. M. 1981. Lipids and the Epidermal Permeability Barrier. *Arch Derm Res*. 270: 95-117.

Elias, P. M. 1983. Epidermal Lipids, Barrier Function, Desquamation. *J Invest Derm*. 80: 44-49.

Elias, P. M. and Barbara E. Brown. 1978. The Mammalian Cutaneous Permeability Barrier. *J Lab Invest*. 39(6): 574-583.

Elias, P. M. and Daniel S. Friend. 1975. The Permeability Barrier in Mammalian Epidermis. *J Cell Biol*. 65: 180-191.

Elias, P. M., Jon Goerke and Daniel S. Friend. 1977. Mammalian Epidermal Barrier Layer Lipids: Composition and Influence on Structure. *J Invest Derm*. 69: 535-546.

Fartasch, M., I.D. Bassukas and T.L. Diepgen. 1993. Structural Relationship Between Epidermal Lipid Lamellae, Lamellar Bodies and Desmosomes in Human Epidermis. *Br J Derm*. 128: 1-9.

Fishman, William H., Kim Kato, C. L. Anstiss and S. Green. 1967. Human Serum ß-Glucuronidase: Its Measurement and Some of its Properties. *Clin Chem Acta*. 15: 435-449.

Fritsch, P., H. Honigsmann and E. Jaschke. 1978. Epidermolytic Hereditary Palmoplantar Keratoderma. *Br J Derm*. 99: 561-568.

Gibbs, R.C. and S.B. Frank. 1966. KHM (Vohwinkel's Syndrome). *Arch Derm*. 94: 619-625.

Goldbarg, James A., E. P. Pineda, B.M. Bank and A. M. Ruthenberg. 1959. A Method for the Colorimetric Determination of ß-Glucuronidase in Serum, Urine, and Tissue. *Gastroenterology*. 36: 193-207.

Goldsmith, Lowell A. 1989. Structure of Skin. *Ultrastruct. Res*. 18: 203-215.

Goodman, Gregory S., Michael B. Sporn and Alfred. B. Roberts. The Retinoids. New York: Academic Press Inc. 1994.

Grayson, Stephen and Peter M. Elias. 1982. Isolation and Lipid Biochemical Characterization of Stratum Corneum Membrane Complexes: Implications for the Cutaneous Permeability Barrier. *J Invest Derm*. 78: 128-135.

Hashimoto, Keito and B. Gross. 1971. Structure and Function of Langerhans Cells. *Arch Derm*. 97: 1101-1126.

Hatamochi, Aiko., Shojiro Nakagawa, Hiroaki Ueki, Kaoru Miyoshi and Iwao Iuchi. 1982. Diffuse Palmo-Plantar Keratoderma with Deafness. *Arch Derm*. 118: 605-607.

Hayashi, Miko, Y. Nakajima and W.H. Fishman. 1964. The Cytologic Demonstration of ß-Glucuronidase Employing Naphthol AS-BI Glucuronide and Hexazonium Pararosanilin: A Preliminary Report. *J Histochem Cytochem*. 12: 293-297.

Hayat, M. A. Fixation for Electron Microscopy. New York: Academic Press Inc. 1981.

Hohl, Daniel. 1990. Cornified Cell Envelope. *Dermatologica*. 180: 201-211.

Hohl, Daniel. 1993. Expression Patterns of Loricrin in Dermatological Disorders. *Am J Dermatopath*. 15(1): 20-27.

Hohl, Daniel., Barbara Ruf Olano, Pierre A. de Viragh, Marcel Huber, Carol J. Detrisac, Urs W. Schnyder and Dennis R. Roop. 1993. Expression Patterns of Loricrin in Various Species and Tissues. *Differentiation*. 54: 25-34.

Hohl, Daniel., Thomas Mehrel, Ulrike Lichti, Maria L. Turner, Dennis R. Roop and Peter M. Steinert. 1991. Characterization of Human Loricrin. *J Biol Chem*. 266(10): 6626-6636.

Hohl, Daniel., Ulrike Lichti, Dirk Breitkreutz, Peter M. Steinert and Dennis R. Roop. 1991. Transcription of the Human Loricrin Gene In Vitro Is Indiced by Calcium and Cell Density and Suppressed by Retinoic Acid. *J Invest Derm*. 96(4): 414-417.

Holbrook, Karen A. and George F. Odland. 1974. Regional Differences in the Thickness (Cell Layers) of the Human Stratum Corneum: An Ultrastructural Analysis. *J Invest Derm*. 62: 415-422.

Humphreys, Walter J. Proceedings of the 7th Annual SEM Symposium. Chicago: IIT Research Institute. 1974.

Hutchens, Lawrence H., Richard W. Sagebiel and Michael A. Clarke. 1971. Langerhans Cell: Structure and Quantitative Distribution. *J Invest Derm*. 56: 325-336.

Ishida-Yamamoto, Akemi., Daniel Hohl, Dennis R. Roop and Robin A. J. Eady. 1993. Loricrin Immunoreactivity in Human Skin: Localization to Specific Granules in Acrosyringia. *Arch Dermatol Res*. 285: 491-498.

Ishida-Yamamoto, Akemi., H. Takahashi and H. Iizuka. 1998. Loricrin and Human Skin Diseases: Molecular Basis of Loricrin Keratodermas. *Histol Histopath*. 13: 819-826.

Ishida-Yamamoto, Akemi and Hajime Iizuka. 1995. Differences in Involucrin Immunolabeling Within Cornified Cell Envelopes in Normal and Psoriatic Epidermis. *J Invest Derm*. 104(3): 391-395.

Ishida-Yamamoto, Akemi and Hajime Iizuka. 1998. Structural Organization of Cornified Cell Envelopes and Alterations in Inherited Skin Disorders. *Exp Derm*. 7: 1-10.

Ishida-Yamamoto, Akemi., Robin A.J. Eady, Fiona M. Watt, Dennis R. Roop, Daniel Hohl and Hajime Iizuka. 1996. Immunoelectron Microscopic Analysis of Cornified Cell Envelope Formation in Normal and Psoriatic Epidermis. *J. Histochem Cytochem*. 44(2): 167-175.

Iwahara, K., Hiro Ogawa and P. Palungwachira. 1992. KHM: Etretinate Treatment and EM Studies. *Austral J Derm*. 1: 19-30.

Juhlin, Lennart., Thierry Magnoldo and Michael Darmon. 1992. Expression of Loricrin in Skin Disorders. *Acta Derm Venereol*. 72: 407-409.

Juhlin, Lennart. and W. Shelley. 1978. The Langerhans Cell: Its Origin, Nature and Function. *Acta Derm*. 79: 7-22.

Kanerva, L., J. Lauharanta and K.M. Niemi. 1983. Electron Microscopic Observations of Mitotic Langerhans Cells as a Possible Sign of Retinoid-Induced Stimulation. *J Cut Path*. 10: 138-143.

Kapur, T.R. and O.P. Singh. 1977. Vohwinkel's Syndrome (KHM). *Ind J Derm*. 43(4): 214-219.

Kikuchi, Ichiro., Takashi Nagata and Shigeo Abe. 1976. Keratosis Palmoplantaris Mutilans. *J Derm*. 3: 85-88.

Klaus, Sidney., Gerald D. Weinstein and Phillip Frost. 1970. Localized Epidermolytic Hyperkeratosis. *Arch Derm*. 101: 272-275.

Korge, Bernhard P., Akemi Ishida-Yamamoto, Claudia Punter, *et al.* 1997. Loricrin Mutation in Vohwinkel's Keratoderma is Unique to the Variant with Ichthyosis. *J Invest Derm*. 109 (4): 604-611.

Krishnaram, Anantrao S., Balam S. N. Reddy, B. R. Garg and A. Bhuvanaratchagan. 1986. Vohwinkel's Disease. *Ind J Derm Ven Lep*. 48: 115-118.

Kustula, U and Linda Orci. 1978. Langerhans Cells of Human Stratum Corneum. *Brit J Derm*. 32: 107-120.

Lampe, Marilyn Anne, Mary L. Williams and Peter M. Elias. 1983. Human Epidermal Lipids: Characterization and Modulations During Differentiation. *J Lipid Res*. 24: 131-140.

Landazuri, Hildebrando. 1991. Keratosis Palmaris et Plantaris and its Surgical Treatment. *J Plas Reconstruct Surg*. 22: 557-561.

Livrea, Michaela and L. Packer. Retinoids. New York: Marcel Dekker Pub. Inc. 1993. pgs. 57-89.

McClung, Ruth. McClung's Handbook of Microscopy Techniques. New York: Hafner Pub. Co. 1967. pgs. 23-119.

Mackenzie, Ian., John R. Bickenback, B. R. Rittman. 1982. Reactivity of Epidermal Cells to a Histochemical Method for the Demonstration of ß-Glucuronidase. *J Invest Derm*. 78: 239-242.

Mackenzie, Joseph C. 1969. Ordered Structure of Mammalian Skin. *Nature*. 222: 881-884.

Maestrini, Elena., Anthony P. Monaco, John A. McGrath, *et al.* 1996. A Molecular Defect in Loricrin, the Major Component of the Cornified Cell Envelope, Underlies Vohwinkel's Syndrome. *Nat Gen*. 13: 70-77.

Magnaldo, Thierry., Francoise Bernerd, Daniel Asselineau and Michel Darmon. 1992. Expression of Loricrin is Negatively Controlled by Retinoic Acid in Human Epidermis Reconstructed In Vitro. *Differentiation*. 49: 39-42.

Maltoltsy, E. G. and P. Parakal. 1965. Membrane Coating Granules of Keratinizing Epithelium. *Cell Biol*. 24: 297-308.

Mehrel, Thomas., Daniel Hohl, Joseph A. Rothnagel, *et al.* 1990. Identification of a Major Keratotinocyte Cell Envelope Protein, Loricrin. *Cell*. 61: 1103-1112.

Menton, David N. and Arthur Z. Eisen. 1971. Structure and Organization of Mammalian Stratum Corneum. *J Invest Derm*. 78: 128-135.

Morris, Jared., A. B. Ackerman and P.J. Koblenzer. 1969. Generalized Spiny Hyperkeratosis. *Arch Derm*. 100: 692-698.

Myers, Samuel. 1990. Lamellar Body Function. *Brit. J Physiol*. 102: 263-267.

Nemanic, Martin K., Jasper S. Whitehead and Peter M. Elias. 1988. Alterations in Membrane Sugars During Epidermal Differentiation: Visualization with Lectins and the Role of Glycosidases. *J Histochem Cytochem*. 31(7): 887-897.

Nielsen, P.G. 1983. Mutilating Palmoplantar Keratoderma. *Acta Derm Venereol*. 63: 365-367.

Nielsen, P.G. 1985. Two Different Clinical and Genetic Forms of Hereditary Palmoplantar Keratoderma. *Clin Gen*. 28: 361-366.

Noriega, Arturo G., Pasquale Ferrera, Roberto Coutiño and Collettte Michalak. 1993. Isolation of an Inhibitor for the Independent M6P-R Endocytosis of Bovine ß-Glucuronidase by Human Fibroblasts. *Arch Biochem Biophys*. 306(2): 331-336.

Onken, Henry D. and Carl A. Moyer. 1963. The Water Barrier in Human Epidermis. *Arch Derm*. 87: 584-590.

Palungwachira, P., K. Iwahara and H. Ogawa. 1992. KHM (Etretinate Treatment and EM Studies). *Austral J Derm*. 33: 19-30.

Peris, K., E.F. Salvati, G. Torlone and S. Chimenti. 1995. KHM (Vohwinkel's Syndrome) Associated with Congenital Deaf-Mutism. *Br J Derm*. 132(4): 617-620.

Postek, M. T., K. S. Howard, A. H. Johnson and K. L. McMichael. SEM: A Student's Handbook. New York: Ladd Research Industries Inc. 1980.

Posthuma, George., Jan W. Slot and Hans J. Geuze. 1987. Usefulness of the Immunogold Technique in the Quantitation of a Soluble Protein in Ulta-thin Sections. *J. Histochem Cytochem*. 35(4): 405-410.

Presley, Norman L. and Frederick J. Bonte. 1981. The Roentgen Appearance of Mutilating Palmoplantar Keratosis. *Am J Roentgen*. 86: 944-949.

Ranvielle, F. and L. M. Tassier. 1975. Studies on the Langerhans Cell. *Dermatologica*. 187: 345-357.

Reams, W.M. and S.P. Tompkins. 1973. A Developmental Study of Murine Epidermal Langerhans Cells. *Dev Biol*. 31: 114-123.

Ricardo-Martinez Jr., I. and Alan Peters. 1971. Membrane Coating Granules and Membrane Modifications in Keratinizing Epithelia. *Am J Anat*. 130: 93-102.

Rhodin, Johannes A.G., An Atlas of Histology. New York: Oxford University Press. 1975. pgs. 273- 297.

Rhodin, Johannes A.G., Histology: A Text and Atlas. New York: Oxford University Press. 1974. pgs. 475- 504.

Rivers, Jason K., E.E. Duke and D.W. Justus. 1985. Etretinate: Management of KHM in Four Family Members. *J Am Acad Derm*. 13: 43-49.

Roop, Dennis R., Christiana K. Cheng, Lynda Titterington, Chester A. Meyers, John R. Stanley, Peter M. Steinert and Stuart H. Yuspa. 1984. Synthetic Peptides Corresponding to Keratin Subunits Elicit Highly Specific Antibodies. *J Biol Chem*. 259(13): 8037-8040.

Rushmer, Robert F., K. Buettner, J.M. Short and George F. Odland. 1966. The Skin. *Science*. 154(3747): 343-348.

Rutenberg, A. M., Ernesto Piñeda, B. M. Banks and J. A. Goldbarger. 1973. Clinical Interpretation of Serum ß-Glucuronidase Activity. *Am J Digest Dis.* 8(10): 789-797.

Schamroth, J.M. 1986. Mutilating Keratoderma. *Int J Derm*. 25: 249-256.

Scheuplein, Richard J. and I. H. Blank. 1971. Permeability of the Skin. *Phys Rev*. 51(4): 702-747.

Sensi, Alejandro, V. M. Bettoli, M. R. Zampino, E. Gandini and E. Calzolari. 1994. Vohwinkel's Syndrome (KHM) and Associated Craniofacial Anomalies. *Am J Med Gen*. 50: 201-203.

Serri, Fernando and William Montagna. 1972. The Structure and Function of Epidermis. *J Invest Derm*. 206: 917-941.

Shelley, Walter B. and Julian Lennart. 1978. The Langerhans Cell: It's Origin, Nature and Function. *Acta Derm Venereol*. 79: 7-22.

Shimuzu, Hiroshi., Akemi Ishida-Yamamoto and Robin A. J. Eady. 1992. The Use of Silver Enhanced Microscopic Localization of Intra- and Extracellular Antigens in the Skin. *J. Histochem Cytochem*. 40(6): 883-888.

Singh, Kamlender. 1986. Mutilating Palmoplantar Keratoderma. *Int J Derm*. 25(7): 436-439.

Smith, Reynaud. Textbook of Pharmacology. Philadelphia: Harcourt Brace Jovanovich, Inc. 1992. pgs. 71-90.

Squier, Charles A., Oberl Fejerskov and A. Jepsen. 1978. The Permeability of Keratinizing Squamous Epithelium in Culture. *J Anat*. 126(1): 103-109.

Staquet, M.J. 1988. Origin and Precursors of the Langerhans Cell. *The Langerhans Cell*. 172: 3-7.

Steinert, P.M. and Marekov, L.N. 1995. The Protein Elafin, Filaggrin, Keratin Intermediate Filaments, Loricrin, and Small Proline-Rich Proteins 1 and 2 Are Isodipeptide Cross-Linked Components of the Human Epidermal Cornified Cell Envelope. *J. Biol. Chem*. 270: 17702-17711.

Steven, A.C., M.E. Bisher, D.R. Roop and P.M. Steinert. 1990. Biosynthetic Pathways of Filaggrin and Loricrin- Two Major Proteins Expressed by Terminally Differentiated Epidermal Keratinocytes. *J Struct. Biol*. 104: 150-162.

Stingl, G. 1980. New Aspects of Langerhans Function. *Int J Derm*. 19: 189-213.

Swartzendruber, Donald C., Philip W. Wertz, David J. Kitko, Kathi C. Madison and Donald T. Downing. 1989. Molecular Models of the Intercellular Lipid Lamellae in Mammalian Stratum Corneum. *J Invest Derm*. 92(2): 251-257.

Sybert, Virginia P., B.A Dale and K.A. Holbrook. 1988. Palmoplantar Keratoderma. *J Am Acad Derm*. 18: 75-86.

Weavers, Andrea., A. Kuhn and G. Mahrle. 1991. Palmoplantar Keratoderma with Tonotubular Keratin. *Am Acad Derm*. 24(4): 638-642.

Wereide, Knut. 1984. Mutilating Palmoplantar Keratoderma Successfully Treated with Etretinate. *Acta Derm Venereol*. 64: 566-569.

Wigley, J.E.M. 1929. A Case of Hyperkeratosis Palmaris et Plantaris Associated with Ainhum-Like Constriction of the Fingers. *J Derm*. 41: 188-191.

Wilgram, George F. and James B. Caufield. 1987. An EM Study of Epidermolytic Hyperkeratosis. *Arch Derm*. 94: 127-143.

Wolff, K. 1972. The Langerhans Cell. *Curr Prob Derm*. 4: 79-145.

Wolff-Schreiner, Elisabeth C. 1987. Ultrastructural Cytochemistry of the Human Epidermis. *Int J Derm*. 16(2): 77-102.

Yeshida, Matsuo K. 1991. ß-Glucuronidase: Origin and Localization. *Int J Biochem*. 269: 1107-1121.

Yoneda, Kozo., Daniel Hohl, O. Wesley McBride, Mary Wang, Kerstin U. Cehrs, William W. Idler and Peter M. Steinert. 1992. The Human Loricrin Gene. *J Biol Chem*. 267(25): 18060-18066.

Yoneda, Kozo., O. Wesley McBride, Bernhard P. Korge, In-Gyu Kim and Peter M. Steinert. 1992. The Cornified Cell Envelope: Loricrin and Transglutaminases. *J Derm*. 19: 761-764.

Zelickson, A. S. 1973. The Langerhans Cell. *J Invest Derm*. 47: 504-514.

Youngstown State University / Youngstown, Ohio 44555-2377
Office of Grants and Sponsored Programs
(216) 742-2377

February 28, 1995

Dr. Paul Peterson
Department of Biological Sciences
U N I V E R S I T Y

Dear Dr. Peterson:

Upon recommendation of the Animal Care and Use Committee, your proposal entitled "Localization of B-Glucuronidase and its Role Among Epithelial Cells of the Skin" (95-003) has been approved.

You must adhere to procedures described in your approved request; any modification must first be authorized by the Animal Care and Use Committee.

Sincerely,

Peter J. Kasvinsky
Dean of Graduate Studies

kb

Enclosure

c: Dr. Leipheimer, Chair, IACUC
Dr. Sobota, Chair, Biological Sciences